Physics – Uspekhi **69** (5) 472 – 500 (2026)

CONFERENCES AND SYMPOSIA

PACS numbers: **75.10. – b,** 75.10.Nr, 75.30.Cr, 75.40.Cx, **75.50. – y**

Griffiths phases and anomalous increase in the Curie temperature in systems with magnetic disorder *

S.V. Demishev, V.V. Brazhkin, A.V. Bokov, O.S. Volkova, R.M. Eremina, V.N. Krasnorussky, I.K. Shamova, A.V. Tsvyashchenko

DOI: https://doi.org/10.3367/UFNe.2025.04.039966

Contents

Abstract. The review considers disordered magnetic systems of the Griffiths type, where the magnetic disorder is caused by the dispersion of local magnetic fields. It is shown that in such systems magnetic clusters exist at temperatures both above and below the Curie point, which leads to an anomalous temperature dependence of the magnetic susceptibility in the paramagnetic phase. A striking manifestation of this type of disorder is the power-law magnetic field dependences of magnetization in the ferromagnetic phase, existing in wide ranges of temperature and magnetic field. The analysis of the parameters of the power-law functions allows constructing the order parameter for the Griffiths phase with a finite magnetic transition temperature. The developed model of magnetic properties is confirmed by experimental results for such strongly correlated systems as manganites, perovskites, cobaltites, dialuminates, pyrochlores, various intermetallics, systems with hidden order and spiral magnets. Recently synthesized substitutional solid solutions in the noncentrosymmetric MnSi–RhSi system are of special interest, as long as in this material the existence of the Griffiths phase is combined with the effect of a giant increase in the Curie temperature up to values of ~ 350 K (12 times with respect to MnSi), exceeding room temperature. This behavior contradicts the standard mechanism of universal suppression of the magnetic transition temperature in the Griffiths phase. To interpret this effect, the spin-polaron model can be used, which considers quasi-bound states of subnanometer size consisting of localized magnetic moments of magnetic ions and itinerant electrons. The analysis of models and experimental data shows that the study of magnetism on the nanometer scale is a promising direction for studying various disordered magnets. The review is based on the materials of the report at the session of the Physical Sciences Division of the Russian Academy of Sciences.

Keywords: Griffiths phase, magnetic disorder, local magnetic fields, ferromagnetic clusters, power-law field dependence of magnetization, noncentrosymmetric magnets, manganese and rhodium monosilicides, giant increase in the Curie temperature, spin polarons

S.V. Demishev [1,a], **V.V. Brazhkin** [1,b], **A.V. Bokov** [1], **O.S. Volkova** [2,c], **R.M. Eremina** [3,d], **V.N. Krasnorussky** [1], **I.K. Shamova** [4,e], **A.V. Tsvyashchenko** [1,f]

[1] Vereshchagin Institute for High Pressure Physics, Russian Academy of Sciences, Kaluzhskoe shosse 14, 108840 Troitsk, Moscow, Russian Federation

[2] Lomonosov Moscow state University, Faculty of Physics, Leninskie gory 1, str. 2, 119991 Moscow, Russian Federation

[3] Zavoisky Physical-Technical Institute, FRC Kazan Scientific Center, Russian Academy of Sciences., Sibirsky tract, 10/7, 420029 Kazan, Russian Federation

[4] National University of Science and Technology MISIS, Leninskii prosp. 4, 119049 Moscow, Russian Federation

E-mail: [a] demishev@hppi.troitsk.ru, [b] brazhkin@hppi.troitsk.ru, [c] os.volkova@yahoo.com, [d] rushana@kfti.knc.ru, [e] m1906776@edu.misis.ru, [f] tsvyash@hppi.troitsk.ru

Received 14 July 2025
Uspekhi Fizicheskikh Nauk **196** (5) 506 – 536 (2026)
Translated by the authors

* This review is based on the report presented for the Scientific Session of the Physical Sciences Division of the Russian Academy of Sciences (PSD RAS), on April 23, 2025 (see *Physics–Uspekhi* **69** (5) 419 (2026); *Uspekhi Fizicheskikh Nauk* **196** (5) 449 (2025)).

1. Introduction

The modification of the magnetic properties of magnets under the influence of doping and disorder can in most cases be understood within the framework of the universal paradigm of the Griffiths phase formation. This phase was theoretically predicted for a model Ising system with the ferromagnetic interaction, in which some of the magnetic bonds are replaced by nonmagnetic ones [1]. In this case, the system is subdivided into ferromagnetic clusters surrounded by a paramagnetic phase, and the ferromagnetic transition occurs at a temperature T_C lower than the Curie temperature of a completely ordered material T_{C0}. In this case, the temperature range $T < T_{C0}$ turns out to be anomalous and is characterized by a nonanalytic magnetization function $M(H, T)$ in terms of magnetic field–temperature variables [1]. Subsequent studies have shown that the Griffiths phase concept is significantly more general and can be applied to magnetic systems of various dimensions with different types of magnetic interaction, both ferromagnetic and antiferromagnetic. It was noted in [2] that the temperature region of anomalies in a disordered magnet is determined not by the temperature T_{C0}, but by a certain temperature T_G, which depends on the distribution function of magnetic bonds, and for a wide distribution function the value of T_G can be infinitely large. If the disorder in the system exceeds some critical value, then the magnetic transition temperature vanishes: $T_C = 0$, and a quantum critical region appears in the magnetic phase diagram [3]. In this case, the Griffiths phase with antiferromagnetic interaction in the limit $T \to 0$ is characterized by anomalous power-law dependences of the magnetic susceptibility $\chi \sim 1/T^{\alpha}$ and the heat capacity $C \sim T^{1-\alpha}$ with the exponent $\alpha < 1$. Experimental observation of such features of $\chi(T)$ and $C(T)$ allows experimental identification of the onset of Griffiths-type quantum criticality [4]. However, in theory, power-law dependences can apparently be strictly obtained only for one-dimensional spin chains [5, 6].

Despite the rather complex theoretical description, the qualitative picture of the magnetic behavior of the system in the Griffiths phase, which follows from the fundamental works [1, 2], seems quite clear [7]. Disorder divides the system into clusters, which can be characterized by different effective values of the magnetic interaction J and the associated local transition temperature T_{Cl}. Temperature T 'scans' the cluster parameters, and for a given value of T, clusters with $T_{Cl} > T$ are disordered, while clusters with $T_{Cl} < T$ are ordered. As the temperature decreases, the enlarged proportion of clusters will be in the magnetically ordered state, and an anomalous temperature dependence of the magnetic susceptibility for the entire system will arise, depending on the distribution function $w(J)$ or $w(T_{Cl})$, and the case $T_C \neq 0$ will obviously correspond to the percolation threshold in a disordered cluster system. To simulate an antiferromagnetic system under quantum critical conditions ($T_C = 0$), it is sufficient to consider a power-law distribution function of the form $w(T_{Cl}) \sim 1/T_{Cl}^{\alpha}$ [7]. This approach not only reproduces the exact results in the limit $T \to 0$, but also allows one to find at an arbitrary temperature the analytical expression for $\chi(T)$, which describes the transition from the Curie–Weiss law at high temperatures $T \gg T_G$ to the power-law dependence $\chi \sim 1/T^{\alpha}$ in the region $T \ll T_G$ in agreement with experimental data [4, 7]. Interestingly, the model under consideration allows one to estimate the cluster size and shows that the Griffiths phase is a nanomagnetic phase [7].

Although the calculation of magnetic characteristics depends on the type of magnetic interaction and disorder, the following general properties hold for any magnet in the Griffiths phase [1–7].

1) The Griffiths phase consists of nanoscale clusters with random parameters, for example, the magnetic transition temperature.

2) Despite the presence of clusters with high local ordering temperatures, $T_{Cl} > T_{C0}$, the uniform magnetic ordering temperature in the system T_C will *always* be lower than the magnetic transition temperature in the absence of disorder, $T_C < T_{C0}$. If the disorder in the magnetic system is sufficiently strong, a quantum critical regime will arise with complete suppression of the magnetic transition temperature.

3) The vicinity of the critical temperature of the system is characterized by anomalous dependences of the magnetic properties, differing from the standard expressions following from mean field theory.

Interestingly, the Griffiths phase paradigm, originally proposed to describe an Ising ferromagnet [1], is currently widely used not only to describe various magnetic materials, including exotic and complex ones, but is also applied in various theoretical models of systems far away from disordered magnets. Examples include Rydberg and ultracold Bose gases [8, 9], logistics problems [10], game theory [11], and the epidemics spread description [12]. However, if we return to various magnetic systems, it turns out that it is the case of the ferromagnetic Griffiths phase that is far from being fully studied, both experimentally and theoretically.

For any magnet, the Griffiths phase paradigm implies a general universal mechanism for suppressing the magnetic transition temperature. However, there are experimental systems with magnetic disorder, which are characterized not only by high magnetic transition temperatures, but also by the effect of enhancing magnetic interaction. Historically, the first such systems were dilute magnetic semiconductors [13, 14], in which doping with magnetic impurities leads to both the formation of the ferromagnetic Griffiths phase [14] and Curie temperatures of ~ 300 K and even higher [13]. Recent studies [15, 16] report the synthesis of a noncentrosymmetric magnet $Mn_{1-x}Rh_xSi$, in which T_C for the Griffiths phase can exceed room temperature, while for the initial undoped material MnSi the Curie temperature is ~ 29 K. We will show that this new system allows us to take a new look at the problem of increasing the ferromagnetic transition temperature in disordered systems. Experimental data for $Mn_{1-x}Rh_xSi$ indicate an intriguing possibility of implementing new mechanisms of magnetic interaction and a giant enhancement of ferromagnetism in cluster systems.

A discussion of doped MnSi would be impossible without at least a brief mention of the rich physics and interesting results associated with this material, including quantum criticality, skyrmion states, the topological Hall effect, and other fascinating phenomena. We have limited ourselves to a few selected references in these areas of research to avoid distracting the reader from the topic of ferromagnetic Griffiths phases with high Curie temperatures, which is the core of our work. We apologize to all researchers whose contributions to these topics were insufficiently mentioned, or not even discussed, despite their widely recognized importance.

This review is based on the lecture presented at a scientific session of the Physical Sciences Division of the Russian Academy of Sciences on April 23, 2025, and is organized as

follows. First, a simple model of the ferromagnetic Griffiths phase will be presented and its implications will be compared with experiment. Next, classical data on MnSi doping will be considered and analyzed within the framework of a developed model approach. Following this, the magnetic properties of $Mn_{1-x}Rh_xSi$ substitutional solid solutions will be analyzed, and the ferromagnetic transition in the Griffiths phase will be described using an experimentally determined order parameter. It is shown that many of the unusual magnetic properties of $Mn_{1-x}Rh_xSi$ may be associated with the formation of spin polarons. The observed gigantic increase in the Curie temperature in the Griffiths phase of $Mn_{1-x}Rh_xSi$ is compared with published data on the effect of negative chemical pressure on the magnetic transition temperature of MnSi and with the results on the enhancement of ferromagnetic interaction in Griffiths phases of dilute magnetic semiconductors. Possible physical mechanisms capable of increasing the Curie temperature and overcoming the universal decrease in the magnetic transition temperature in the Griffiths phase are discussed.

2. The model of the Griffiths ferromagnetic phase

Let us consider a Griffiths-type magnet consisting of clusters characterized by a set of random parameters including the exchange integral J, the magnetic transition temperature T_{Cl}, the local field $\mathbf{H}_l$, and the saturated magnetization $\mathbf{M}_0$ (Fig. 1). For any parameter, in the general case, it is necessary to specify a certain distribution function $w(J)$, $w(T_{Cl})$, $w(\mathbf{H}_l)$ and $w(\mathbf{M}_0)$. The magnetization of each cluster $\mathbf{M}$ depends both on the external magnetic field $\mathbf{H}$ and on the local field $\mathbf{H}_l$ generated by all clusters in the system. One can expect that one or another type of disorder will dominate in different experimental systems. A rigorous theory should start with the distribution of exchange energies J and take into account the correlations associated with the cluster size, i.e., with the parameter $\mathbf{M}_0$ [1,2]. However, in this case, exact results can be obtained for special spin systems in the limit $T \to 0$ [2, 5, 6]. To obtain a simple but realistic model, the distribution of J can be replaced by a similar distribution of transition temperatures T_{Cl} [7]. For example, one can imagine a situation where the clusters are weakly magnetic, resulting in a small amplitude of the local fields, $H_l \ll H$, and the main disorder is associated with the spread of T_{Cl} and M_0. This situation corresponds to the description of the classical Griffiths phase at a qualitative level [1, 2], takes into account the arguments of [2], and, obviously, most closely corresponds to the case of disordered antiferromagnets. Under the simplifying assumption $M_0 = \text{const}$ (the sample is divided into cells with the same number of spins), for the model allowing a good description of the experimental data for the quantum critical regime with a completely suppressed magnetic transition $T_C = 0$, it is sufficient to take into account the distribution $w(T_{Cl})$ [4, 7].

Another limiting case appears when the critical magnetic transition temperature T_C is well defined and nonzero. Then the main disorder in the cluster system is associated with random local fields $\mathbf{H}_l$. Physically, such a situation can arise for ferromagnetic clusters and, therefore, should correspond to the ferromagnetic Griffiths phase. However, despite the fact that the Griffiths phase was initially proposed specially for the ferromagnetic case [1], this type of disorder at the 'strict' level has apparently not been sufficiently studied [16–20]. Therefore, simple models that take this type of disorder into account are of special interest [16, 18].

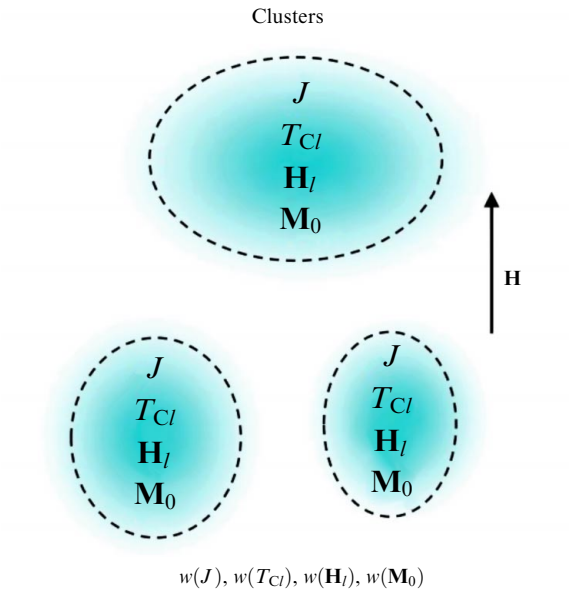

Figure 1. A disordered Griffiths-type magnet consisting of clusters with random values of exchange energy J, saturation magnetization $\mathbf{M}_0$, Curie temperature T_{Cl} and local magnetic field $\mathbf{H}_l$.

We suppose that in a cluster system the total magnetization $\mathbf{M}$ is parallel to the external magnetic field $\mathbf{H}$, i.e., the projections of the local field $\mathbf{H}_l$ perpendicular to the vector $\mathbf{H}$ always cancel out each other. If such compensation is assumed at the level of each cluster, then it is sufficient to take into account the dispersion of the component of the local field H_l parallel to the external magnetic field. As in the approach adopted in [7], we initially neglect the dispersion of $\mathbf{M}_0$ and consider clusters of the same size.

Then, to describe the magnetization of a cluster in a disordered phase, we can use the expression

$$M = M_0 \varphi \left(B_0(T)(H + H_l) \right), \qquad (1)$$

where $\varphi(x)$ defines the field dependence of the cluster magnetization and has asymptotic behavior $\varphi(x) \sim x$ at $x \to 0$, and $\varphi(x) \to 1$, at $x \to \infty$. When performing calculations, one of the standard functions describing the magnetization of a paramagnet should be chosen as $\varphi(x)$. For example, in [19, 20], when considering a cluster system in the ferromagnetic Griffiths phase, approximations $\varphi(x) = \tanh(x)$ (the Brillouin function for spin $S = 1/2$) and $\varphi(x) = L(x)$ (the Langevin function for classical magnetic dipoles, $S \to \infty$) were used. In the temperature range $T > T_C$, the parameter B_0 can be chosen in the model form: $B_0 = \mu^*/k_B(T - T_C)$, where μ^* is the effective magnetic moment [21]. For a cluster in a ferromagnetic state at $T < T_C$, we can set $B_0 \to \infty$, and in this case the function $\varphi(z)$ will take the universal form: $\varphi(z) = \text{sgn}(z)$.

As long as the dispersion of T_C can be neglected according to the above assumption, it follows that the dispersion of B_0 does not need to be taken into account, and the resulting magnetic response of a system consisting of clusters can be found by averaging expression (1) taking into account the corresponding distribution function $w(H_l)$ [16, 18]. Physically, this situation corresponds to the case when the magnetic transition at $T = T_C$ in a system with disorder is preserved,

although it can occur at a temperature lower than for a completely ordered system.

Thus, in our model, the main disorder is associated with the dispersion of local magnetic fields. Let us consider the case where the distribution of local fields is given by a power function

$$w(H_l) = \frac{1-\xi}{2H_{\rm m}^{1-\xi}|H_l|^{\xi}}\,, \quad |H_l| \leqslant H_{\rm m}\,, \quad \xi < 1\,, \tag{2}$$

satisfying the normalization condition

$$\int_{-H_{\rm m}}^{H_{\rm m}} w(H_l)\,{\rm d}H_l = 1\,. \tag{2a}$$

In Equations (2) and (2a), the field $H_{\rm m}$ corresponds to the formally introduced cutoff field, which ensures the finite value of the integral (2a). For the assumptions made, the magnetic response of the cluster system in the case under consideration can be represented in the form [16, 18]:

$$M = M_0 \int_{-H_{\rm m}}^{H_{\rm m}} w(H_l)\,\varphi\big(B_0(H+H_l)\big)\,{\rm d}H_l\,. \tag{3}$$

Let us introduce the dimensionless variables $x_0 = H/H_{\rm m}$, $x_l = H_l/H_{\rm m}$, $m = M/M_0$ and $a = B_0 H_{\rm m}$. Then from Eqns (2) and (3) we obtain

$$m(x_0) = \frac{1-\xi}{2}\int_{-1}^{1} \frac{\varphi\big(a(x_0+x_l)\big)}{|x_l|^{\xi}}\,{\rm d}x_l\,, \tag{4}$$

and finding the magnetic properties of a model cluster system is reduced to calculating the integral (4).

When using model functions of the type $\varphi(x) = \tanh(x)$ or $\varphi(x) = L(x)$ it is impossible to obtain analytical expressions for the field dependence of the reduced magnetization $m(x_0)$ using Eqn (4). However, as was shown in [18], this difficulty can be circumvented if a piecewise continuous approximation is used instead of the Brillouin type $\varphi(x)$

$$\varphi(x_0) = ax_0\,, \quad ax_0 < 1\,, \tag{5a}$$

$$\varphi(x_0) = 1\,, \quad ax_0 \geqslant 1\,, \tag{5b}$$

which for a cluster in a ferromagnetic state will be reduced to the step-type function considered above

$$\varphi(x_0) = {\rm sgn}\,(x_0)\,. \tag{6}$$

At first glance, from a comparison of the functions $\varphi(x_0) = \tanh(ax_0)$ (Fig. 2a, curve *1*) and the piecewise continuous function (5) with the same slope for $x_0 \ll 1$ (Fig. 2a, curve *2*), it follows that function (5) gives too rough an approximation. Indeed, for $x_0 = 1$ the difference reaches 24%. We consider this issue in more detail following the work [18]. As can be seen from Fig. 2b, in the integrand in formula (4) for small x_0, the region of the possible maximum difference between $\varphi(x) = \tanh(ax)$ and approximation (5) will fall on small values of $w(x)$ and, as a result, the error in calculating $m(x_0)$ will be significantly smaller compared to the difference in the values of the functions mentioned above. Direct numerical calculation confirms this assumption, and in the region $T > T_{\rm C}$, the considered model expressions for the cluster magnetization give values of $m(x_0)$ that differ by no more than 2–5%. Thus, using functions (5) and (6) does indeed make it possible to obtain analytical results with acceptable accuracy. Note that for $T < T_{\rm C}$, the $\varphi(x_0) = \tanh(ax_0)$ type function and piecewise continuous approximation are reduced to the same expression (6).

For further analysis, the following three situations are of greatest interest. The first case is small values of a, $a \ll 1$, when the function $\varphi(x)$ is linear in the entire region of integration over x_l in Eqn (4) (Fig. 2b, curves *1*, *2*). The next case is intermediate values of a, $a \geqslant 1$ for which the nonlinear nature of $\varphi(x)$ must be taken into account (Fig. 2b, curves *3*, *4*). And, finally, the limiting ferromagnetic case $a \gg 1$, when $\varphi(x)$ degenerates into a step (Fig. 2b, curve *5*). Calculating the integral (4) using the piecewise continuous approximation (5) and function (6) yields the following analytical expressions [16, 18]:

$$m = ax_0\,(a \ll 1)\,, \tag{7}$$

$$m = a^{\xi}x_0 + O(x_0^3)\,(a \geqslant 1)\,, \tag{8}$$

$$m = x_0^{1-\xi}\,(a \gg 1)\,. \tag{9}$$

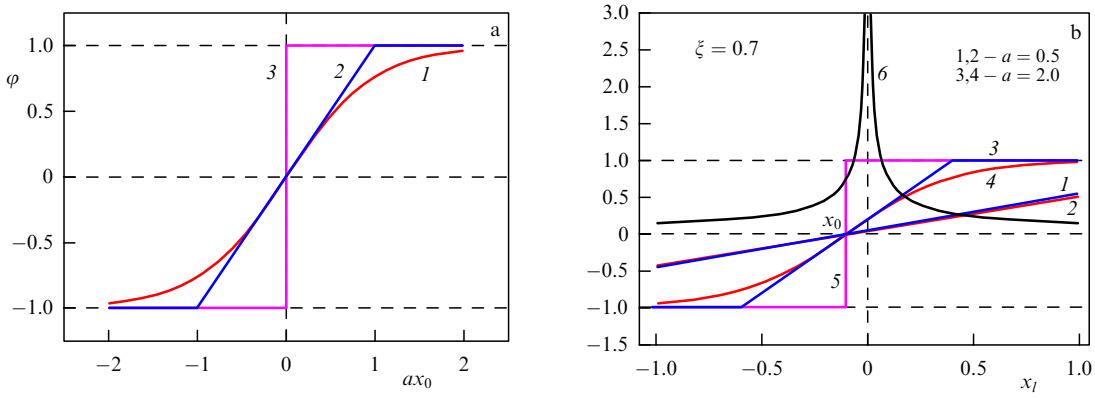

Figure 2. (a) Comparison of various approximations for the function describing the cluster magnetization. *1* — $\varphi(x) = \tanh(ax_0)$; *2* — piecewise continuous function, Eqns (5a) and (5b); *3* — the case of a ferromagnetic cluster (Eqn (6)). (b) Functions included in the integrand in formula (4). Curves *1–5* — correspond to various approximations for $\varphi(x)$. Curve *6* represents the distribution function (2) for the reduced local field $w(x_l) = (1-\xi)/2|x_l|^{\xi}$. *1*, *3* — piecewise continuous approximation (5) for different values of the parameter a, *2*, *4* — function $\varphi(x) = \tanh(ax_0)$, taken with the same slope at zero as function (5). Curve (*5*) corresponds to the ferromagnetic case (Eqn (6)). Curves *1*, *2* and *3*, *4* are plotted for values $a = 0.5$ and $a = 2$, respectively. The function $w(x_l)$ is given for the exponent $\xi = 0.7$. (From the work [18].)

The obtained relations (7) and (8) correspond to the region of a linear magnetic response with respect to the field at $T > T_C$, and Eqn (9) describes the nonlinear dependence of magnetization in the ferromagnetic region ($T < T_C$). In this case, the power-law asymptotic (9) is fulfilled up to $x_0 = 1$, and in the range $x_0 \geqslant 1$, the magnetization saturates: $m \equiv 1$.

Let us move on to dimensional variables. Then, from (7), (8), it is easy to find expressions for the magnetic susceptibility $\chi = M/H$:

$$\chi = M_0 B_0 = \frac{M_0 \mu^*}{k_B(T - T_C)}, \quad \left(\frac{\mu^* H_m}{k_B(T - T_C)} \ll 1\right), \qquad (10)$$

and

$$\chi = \frac{M_0}{H_m}\left(\frac{\mu^* H_m}{k_B(T - T_C)}\right)^{\xi}, \quad \left(\frac{\mu^* H_m}{k_B(T - T_C)} \geqslant 1\right). \qquad (11)$$

Thus, at $T \gg T_C$, the Curie–Weiss law (10) will be valid, and as the Curie temperature is approached, the denominator in formulas (10) and (11) will decrease (the dimensionless parameter a will increase) and, consequently, in some vicinity of the Curie temperature, an anomalous magnetic 'Griffiths' susceptibility (11) will arise. The crossover between the considered asymptotics will occur at $a = 1$, i.e., at a temperature T_{cr} equal to $T_{cr} = T_C + \Delta T$, where $\Delta T = \mu^* H_m / k_B$. The characteristic temperature T_{cr} can be found from experiment, and its value can be used to estimate the model parameter, the cutoff field H_m.

It should be noted that the transition from Eqn (10) to Eqn (11) occurs within the same local field distribution function (2) and is not associated with the emergence of any specific correlations. This result is entirely consistent with the analysis of the Griffiths phase performed in the classical work [2]. In it, attention was drawn to the fact that the distribution function of the parameters of the clusters forming the Griffiths phase exists at any temperature and, in the strict sense, the entire paramagnetic region of a disordered magnet should be considered as anomalous one.

In dimensional variables, the power field dependence for $H < H_m$ magnetization (9) has the form

$$M = M_0\left(\frac{H}{H_m}\right)^{1-\xi}, \qquad (12)$$

and in the region $H \geqslant H_m$ the saturation occurs: $M = M_0$. This type of magnetic behavior is a consequence of two factors: the universal power-law distribution function of local magnetic fields and the sharp dependence of the magnetization of each cluster on the magnetic field. The magnetic response of each cluster fits into the conventional paradigm used to describe a ferromagnet, while the specific dependence (12) arises as a result of the influence of disorder on the magnetic subsystem.

If dependence (12) is satisfied, then most clusters are in a ferromagnetic state, and their magnetization is described by Eqn (6). Therefore, within the framework of our model, an anomalous power-law dependence of magnetization can arise in a certain temperature range below the Curie temperature, and as the Curie point is approached from below from the ferromagnetic region, the asymptotic dependence (12) may be violated.

Note that for approximation (6), the above constraint on the constancy of M_0 can be lifted. If the random variables M_0 and H_l are independent, then averaging with the distribution function (2) for H_l and any distribution function M_0 will again lead to formula (12), in which M_0 will be the average magnetization of the cluster. Since at $T < T_C$ the value of M_0 specifies the spontaneous magnetization of clusters, it can play the role of an order parameter, and a critical temperature dependence of the form can be expected for it:

$$M_0 \sim (T_C - T)^{\beta}. \qquad (13)$$

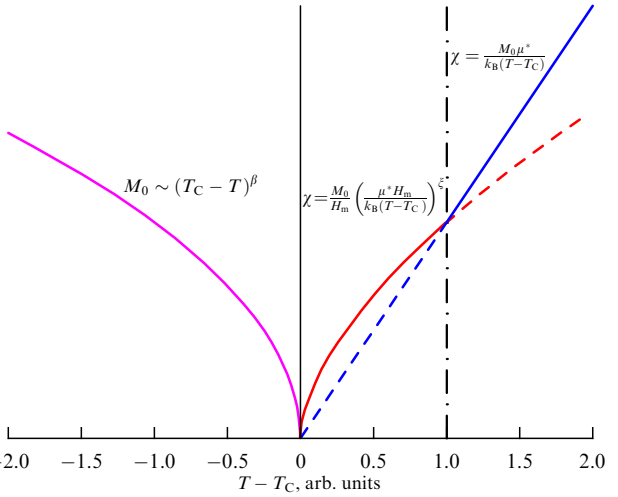

Figure 3. Properties of the model of a disordered cluster ferromagnetic phase: change in the asymptotic behavior of the inverse magnetic susceptibility ($T > T_C$) and the order parameter ($T < T_C$).

Obviously, in the case where the possible temperature dependences $\xi(T)$ and $H_m(T)$ do not have a critical singularity at the Curie point and are not too strong, the temperature dependence of the coefficient of $H^{1-\xi}$ in the field dependence $M(H)$ may be used to estimate the temperature dependence of the order parameter from experimental data. The change in magnetic characteristics following from the considered model is shown in Fig. 3.

Note that in a real ferromagnetic cluster system, the distribution of local fields is a consequence of the dispersion of cluster magnetizations and depends on their shape, relative position, and size. Since at least the cluster magnetization is a function of temperature, a temperature-dependent distribution function (2) with $\xi(T)$ and $H_m(T)$ may be expected. As a result, the exponent $\alpha(T) = \xi(T)$ in the power law is generally not universal. It cannot be ruled out that in some systems, the $\xi(T)$ and $H_m(T)$ dependences may be strong and so significant that they determine the observed features of the magnetic characteristics. In this case, using the field dependence (12) to find the temperature dependence of the order parameter will be difficult.

In the model under consideration, the power-law dependence $M(H)$ may be observed over a wide temperature range $T < T_C$. This result differs radically from the behavior expected for a ferromagnet with the standard equation of state. In this case, the power-law dependence $M(H)$ can appear *only* at the Curie point $T = T_C$ [22], and the exponent will be universal $M \sim H^{1/(\gamma/\beta+1)}$, depending on the critical indices for the susceptibility γ and the order parameter β. In Landau theory, $\gamma = 1$ and $\beta = 1/2$; therefore, the relation $M \sim H^{1/3}$ should be satisfied [22]. We emphasize once again that the features of the magnetic properties expected in the

model under consideration are not associated with the anomalous behavior of the magnetization of an individual cluster, but arise as a result of the disorder-induced modification of the integral characteristics of the Griffiths system.

In the next section, experimental examples will be given. They show that, despite the extreme simplicity of the model of a disordered cluster ferromagnetic phase with disorder determined by random local magnetic fields with a power-law distribution function, this approach allows one to analytically describe from a unified point of view the experimentally known magnetic properties of the systems, commonly referred to in the literature as Griffiths ferromagnetic phases.

3. The Griffiths ferromagnetic phase. Experimental data

Although the fundamental theoretical work [1] on the physics of the Griffiths phases was published more than half a century ago, the first experimental studies in this area appeared significantly later, around the early 2000s. We will be interested primarily in the properties of the Griffiths phase in ferromagnetic systems. Note that in this case, the experimental data correspond to the case of $T_C \neq 0$, which differs radically from systems with antiferromagnetic interaction, where it is possible to observe the Griffiths quantum critical regime with a transition temperature completely suppressed by disorder [4]. Therefore, in disordered ferromagnets, primary attention is paid to the behavior of magnetic properties in the paramagnetic phase [20, 23–37]. The set of experimental objects is distinguished by significant diversity and includes manganites [23, 24, 31], perovskites [29, 30], cobaltites [32], dialuminates [27, 28], pyrochlores [34], various intermetallics [20, 25, 26, 33, 36, 37] and even such exotic systems with hidden order as URu_2Si_2 [35]. The disorder necessary for the emergence of the Griffiths phase in most studies is associated with various impurities replacing the original elements in the crystal structure or with its defects.

It is reliably established that in the region of the linear magnetic response in the paramagnetic phase ($T > T_C$), the magnetic susceptibility χ of a disordered Griffiths-type ferromagnet is described by following Equation [23–34]:

$$\chi(T) \sim \frac{1}{(T - T_C)^{1-\lambda}}, \qquad (14)$$

and both the situations with $\lambda = 0$ (Curie–Weiss law) and with $\lambda \neq 0$ ($\lambda < 1$) are possible. In this case, the Curie–Weiss law ($\lambda = 0$) is valid far from the magnetic transition point, and as the temperature decreases and approaches T_C, an anomalous power-law dependence ($\lambda \neq 0$) arises. The temperature at which the exponent changes from $\lambda = 0$ to $\lambda \neq 0$ is often interpreted as a transition to the Griffiths phase, $T \sim T_G$, and the region of existence of the Griffiths phase is understood as the interval $T_C \leqslant T \leqslant T_G$. Note that in the standard theory of phase transitions $\chi \sim |T - T_C|^{-\gamma}$, where the critical index γ is either equal to unity (mean field theory, Landau theory), or is greater than unity in most models (for example, in the Heisenberg and Ising models, in the $X-Y$ model and the spherical model) (see [38], p. 43 of Russian edition). This circumstance confirms that the Griffiths phase is a special case to which the standard theory of phase transitions is hardly applicable.

It is interesting that the values of $\lambda \neq 0$ ($\lambda < 1$) observed together with a finite temperature T_C do not have a completely satisfactory theoretical justification, despite the citation of sources in [23–34]. As a rule, the work [39] is cited as the primary source; however, having opened it, it is easy to see that in [39] the discussion is about the dependence of the magnetic susceptibility of the type $\chi \sim 1/T^{\xi}$ in the limit $T \to 0$, i.e. the quantum critical regime with a completely suppressed magnetic transition temperature $T_C = 0$. Obviously, a certain amount of courage is required to extend this asymptotically exact result to formula (14), which is valid in three-dimensional systems such as manganites, in the vicinity of $T_C = 200-270$ K [23, 24, 31].

The considered variant of magnetic data analysis in the Griffiths systems is distinguished by its extreme simplicity, which, apparently, predetermined its use in the overwhelming majority of studies. In all fairness, it should be noted that a more correct approach to the identification of the ferromagnetic Griffiths phase is also presented in the literature, based on the consideration of the Lee and Yang zeros [40, 41]. However, the data analysis method used in [40, 41] turned out to be too complex for the experimentalists and, as a result, was 'defeated' by the simple approach described above. Interestingly, in [40, 41] the 'Griffiths' formula for $\chi(T)$ [14] is also postulated without any justification.

Thus, we see that in the region $T > T_C$ the only consistent description of the transition from the Curie–Weiss law for magnetic susceptibility to the power-law dependence (14) with $\lambda \neq 0$ is the phenomenological model considered in the previous section, in which we must set $\xi = 1 - \lambda$ (see Eqns (11) and (14)). At first glance, if we limit ourselves to a qualitative analysis of the results available in the literature, then its predictions for the paramagnetic phase (Fig. 3) are in perfect agreement with experiment. However, this is not entirely true, and, as follows from Fig. 4, several different variants of the transition from dependence (14) with $\lambda = 0$ to dependence (14) with $\lambda \neq 0$ are presented in the literature. Firstly, there are systems [23] for which the temperature dependence of the magnetic susceptibility is in good agreement with the predictions of the model with dispersion of the local magnetic field (Fig. 4a, where the linear dependence *1* describes the Curie–Weiss law and curve *2* corresponds to the theoretical dependence (11)). Secondly, a case is possible [29] when Eqn (11) with $\xi < 1$ is satisfied with good accuracy in the entire studied temperature range (Fig. 4b), and to resolve the issue of the applicability of the considered model, additional studies at higher temperatures are required.

It is interesting to compare the situation similar to Fig. 4b with the results of the traditional analysis, which declares the observation of the transition $\lambda = 0 \to \lambda \neq 0$ at $T \sim T_G$. The comparison shows that in some systems [30] the limited temperature range in which the magnetic measurements were carried out does indeed lead to an ambiguous interpretation. On the one hand, the theoretical dependence (11) with $\xi = 0.66$ is in good agreement with the experiment over a wide temperature range, and in the vicinity of $T_C \sim 180$ K there is a broadening of the transition region due to the influence of fluctuations (Fig. 4c, curve *2*). However, if desired, a high-temperature linear region can be distinguished on the $\chi^{-1} = f(T)$ curve (Fig. 4c, curve *3*) with a characteristic temperature $T_C \sim 127$ K, which is *lower* than the transition temperature following from the analysis using the power-law dependence (11) (Fig. 4c, curves *2* and *3*). This type of $\chi(T)$ data is often encountered in the literature, when

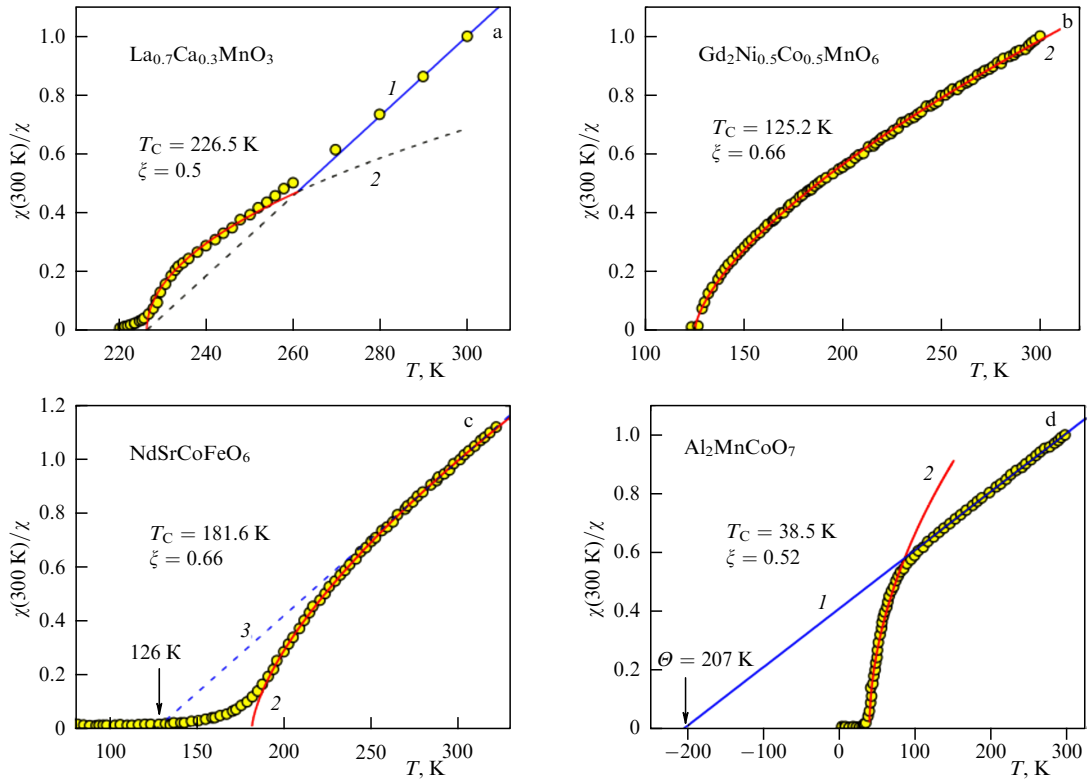

Figure 4. Comparison of the temperature dependence of the inverse magnetic susceptibility in various materials with the predictions of the Griffiths cluster model of the ferromagnetic phase. The dots represent experimental data from [23] (panel a), [29] (panel b), [30] (panel c), and [34] (panel d). The numbers indicate: *1* — the Curie–Weiss law (Eqn (10); *2* — the power-law temperature dependence of the magnetic susceptibility (Eqn (11)). In the panel c, the dotted line 3 denotes the extrapolation of the possible high-temperature 'linear' section of the $\chi^{-1}(T)$ curve (see text).

the formation of the Griffiths phase at $T = T_G$ is associated with a downward deviation from the linear section of the $\chi^{-1} = f(T)$ curve [42, 20, 23–37]. In particular, for the data shown in Fig. 4c, the transition from the paramagnetic phase to the Griffiths phase is expected at $T_G \sim 250$ K.

However, it is easy to see that this method of data analysis and interpretation is poorly consistent with the qualitative picture of the ferromagnetic Griffiths phase. If we assume that correlations in the paramagnetic region are insignificant, then disorder should have a weak effect on the paramagnetic temperature in the Curie–Weiss law. Consequently, the temperature T_C, determined from extrapolation of the linear high-temperature portion of the $\chi^{-1} = f(T)$ curve, should be close to the Curie temperature in a completely ordered system, i.e., higher than the Curie temperature in the Griffiths phase, since magnetic disorder reduces the magnetic transition temperature. However, as can be seen from the example shown in Fig. 4c, the actual situation is exactly the opposite.

Nevertheless, experimental examples of the formation of the Griffiths phase — when the dependence $\chi^{-1} = f(T)$ with a downward deviation from the linear region arises in the paramagnetic phase — are quite numerous and contradict the behavior expected in the model considered above, when the inverse magnetic susceptibility in the region of the power-law temperature asymptotics (11) turns out to be greater than the values extrapolated from the linear region (see Fig. 3). In our opinion, the discrepancy between theory and experiment may be associated with the more complex nature of the magnetic interaction in real magnets with disorder. For example, from Fig. 4d it follows that in the Al_2MnCoO_7 compound [34] the extended Curie–Weiss region corresponds to the dominant antiferromagnetic interaction with a paramagnetic temperature of $\Theta \simeq 200$ K (Fig. 4d, curve *1*), against the background of which a temperature dependence of the magnetic susceptibility typical of the ferromagnetic Griffiths phase arises (Fig. 4d, curve *2*). Such a crossover between the antiferromagnetic and ferromagnetic types of temperature dependence of the magnetic susceptibility is well known for various strongly correlated systems and was observed, for example, in the heavy-fermion metal CeB_6 [43] and vanadium oxide nanomaterials [44]. Thus, we assume that the common scenario with a downward deviation from the linear region indicates the presence of several types of magnetic interactions in the system, when the antiferromagnetic interaction leads to an additional decrease in the paramagnetic temperature. At the same time, the considered model takes into account only the ferromagnetic interaction and, therefore, can be guaranteed to describe the temperature dependence of the magnetic susceptibility (11) in the vicinity of T_C, where ferromagnetism and disorder effects dominate.

Another important consequence of the cluster model with a power-law distribution function of local fields is the anomalous power-law dependence of magnetization on the magnetic field (12). In experiments, a dependence of the form $M \sim H^{\alpha}$ with the exponent α less than unity, not associated with the Curie point, has been repeatedly observed in various systems [20, 35–37], although this type of magnetic behavior has received significantly less attention compared to the features of magnetic susceptibility in the vicinity of T_C. In the existing literature, the power-law field dependence of magnetization is unambiguously associated with the Grif-

fiths phase, although without rigorous justification. This conclusion is based on the analogy with the asymptotically exact results at $T \to 0$, which can be obtained, for example, for one-dimensional ferromagnetic spin chains in the Griffiths phase [5, 6]. At a qualitative level, this assumption can be explained as follows: a quantum critical Griffiths system can be formally described as a system with $T_C = 0$, for which, as in a classical ferromagnet, a power-law dependence $M(H)$ will arise in the vicinity of T_C, i.e., in this case, at $T \to T_C = 0$. However, the possibility of extending this result to the region of finite temperatures before establishing the cluster model with a power-law distribution function of local fields [16, 18] had no justification.

Anomalous behavior of magnetization of the type $M \sim H^{\alpha}$ was observed in a compound with itinerant magnetism URu_2Si_2. In [35], it was shown that the phase with hidden order in this material, arising in the region $T < T_{ho} \sim 17.5$ K, can be considered as a Griffiths cluster phase of the ferromagnetic type with $T_G = T_{ho}$. In this case, the disorder necessary for observing Griffiths anomalies can apparently be associated with defects in the crystal structure and complex magnetic interactions leading to a disordered distribution of the spin density in the bulk of the sample, equivalent to the partition of a Heisenberg-type system into magnetic clusters [35]. Note that itinerant magnetism does not exclude the Griffiths type of behavior, which has not only been repeatedly observed in such systems, but is also well substantiated theoretically [45].

It is interesting that for URu_2Si_2 for $T > T_{ho}$ the field dependence in the range $H < 9$ T is linear ($\alpha \equiv 1$), as it should be for an itinerant magnet, and upon transition to the phase with hidden order ($T < T_{ho}$) in the same range of magnetic field the magnetization begins to change with the magnetic field according to the power law $M \sim H^{\alpha}$. The exponent for $T < T_{ho}$ is a function of temperature and is close to unity, but slightly less than this value: $\alpha = 0.98-0.92$. It is easy to see that this result is in reasonable agreement with the behavior expected in the considered cluster model of the Griffiths ferromagnetic phase, where $\alpha = 1 - \xi$ (see Section 2).

In [20], samples of $Co_{1+x}Sn$ alloys were investigated in the composition range of $0.45 \leqslant x \leqslant 1$. Excess cobalt in this system stabilizes the hexagonal crystal structure of the $B8_1$ type. Field dependences of magnetization were studied in the range $H < 7$ T and it was shown that the Griffiths phase is formed in compositions with $x = 0.45-0.65$. At $T = 10$ K, a power-law dependence $M \sim H^{\alpha}$ is observed with an exponent depending on the cobalt content and taking values from the range $\alpha = 0.7-0.2$, and the value of α decreases with increasing x [20]. The authors of [20] did not estimate the temperature of the transition to the Griffiths phase, but noted that for compositions in the range $x = 0.45-0.65 \leqslant x \leqslant 1$, clusters with excess cobalt content form a ferromagnetic phase as a result of their merging into a single infinite cluster. This phase, formed as a result of the percolation transition, has Curie temperatures exceeding ~ 600 K [20]. From the point of view of the cluster model considered in the previous section, the temperature of the ferromagnetic transition in clusters should be sufficiently high and correspond in order of magnitude to the Curie temperature for the entire sample. Therefore, the temperature $T \sim 10$ K at which the field dependences of magnetization were studied should lie in the ferromagnetic region of the Griffiths type, and the results of [20] can be considered as experimental confirmation of the considered model approach.

Nontrivial magnetic behavior was discovered in the $Ni_{1-x}V_x$ system with $x \leqslant 15\%$ [36, 37]. In this intermetallic compound, an increase in vanadium concentration leads to a decrease in T_C, and at $x_c \sim 11.6\%$, the Curie temperature, with experimental accuracy, turns to zero, thus leading to a transition to the quantum critical regime. In the region $x < x_c$, where the Curie temperature is finite, at low temperature $T = 2$ K$< T_C(x)$, two contributions could be distinguished in the field dependence of magnetization; the first one gives a magnetization $M_{sat} = \text{const}$, saturating in a field $H > 1-2$ kOe, and the second is a function $M \sim H^{\alpha}$ with an exponent $\alpha = 0.8-0.2$ depending on the composition. In this case, the authors of [36, 37] associate the power-law contribution to the total field dependence, observed in the entire studied range of $H < 50$ kOe, with the Griffiths phase existing within the ferromagnetic phase described by ordinary saturated magnetization.

This feature of magnetic behavior can be easily interpreted within the framework of a cluster model with local field dispersion, assuming significant heterogeneity of the $Ni_{1-x}V_x$ samples, characterized by regions with closely spaced ferromagnetic clusters with excess nickel and paramagnetic regions dominated by a phase with low nickel content. The influence of ferromagnetic clusters on the paramagnetic phase is small, while the mutual influence of closely spaced magnetic clusters can lead to dispersion of local fields, for example, of a power-law type. Then, the saturating contribution will be associated with the paramagnetic phase, and the disordered phase of interacting ferromagnetic clusters will exhibit a power-law dependence $M \sim H^{\alpha}$ (see Eqn (12)).

In the concentration range $x > x_c$, the magnetic system of $Ni_{1-x}V_x$ turns out to be highly diluted and highly disordered. In this case, $T_C \approx 0$ (in the experiment, $T_C < 0.1$ K [36]) and the saturating contribution with M_{sat} disappears, while the power-law dependence $M \sim H^{\alpha}$ is preserved. It is easy to see that the model approach considered in the previous section has no limitation on the value of T_C, and within this framework, only the ferromagnetic response of each cluster and the distribution function of local fields are significant. From this point of view, the magnetic system of $Ni_{1-x}V_x$ at $x > x_c$ consists of ferromagnetic clusters, the distribution of which over the volume of the sample is more homogeneous, resulting in a dependence of the magnetization on the magnetic field given by Eqn (12): $M \sim H^{1-\xi}$. In the limit of small T_C, Eqn (11) reduces to an asymptotic power-law behavior: $\chi \sim 1/T^{\xi}$. Thus, if our model is valid, then the exponent ξ for the low-temperature asymptotic behavior of the magnetic susceptibility and the exponent of the field dependence of magnetization α should be linked by the obvious relation $\alpha = 1 - \xi$. Interestingly, exactly this relation between the exponents was experimentally discovered in [36].

To sum up, it can be concluded that the results of works [36, 37] for the $Ni_{1-x}V_x$ system are in good agreement with the model [16, 18] of the Griffiths ferromagnetic phase, which naturally allows one to explain the nature of the occurrence of the anomalous power-law field dependences of magnetization. However, as in the case of work [20], in [36, 37] possible anomalies of magnetic susceptibility in the paramagnetic phase were not considered, and a complete verification of theoretical predictions using the example of these systems is impossible. The opposite situation is characteristic of the studies carried out in [23–34], where the main attention was paid to the $\chi(T)$ data in the region $T > T_C$, and the question

of the existence of power-law dependences $M \sim H^{\alpha}$ in the ferromagnetic region $T < T_C$ has not yet been studied. However, an analysis of the experimental situation allows one to conclude that a simple cluster model [16, 18] provides a reasonable description of the set of anomalies of magnetic properties characteristic of the Griffiths ferromagnetic phases.

Within the framework of the approach used, the Griffiths phase can be considered as a set of correlated clusters (in our case with ferromagnetic interaction) and a paramagnetic phase filling the space between the clusters. As shown in a recent review [42], this understanding of the Griffiths ferromagnetic system is confirmed by electron paramagnetic resonance (EPR) data.

In the presence of ferromagnetic regions 'embedded' in the paramagnetic phase, one can expect both a complex magnetic resonance spectrum and a distortion of the absorption line shape. Depending on the magnitude of the internal magnetic fields and the shape of the ferromagnetic regions, one can expect the appearance of several ferromagnetic lines. This effect is manifested in the EPR spectra of manganites in the X-band [46], and the ferromagnetic resonance (FMR) lines, as a rule, can coexist with the paramagnetic resonance (PMR) lines [42]. This behavior reflects the coexistence of short-range magnetic correlations in ferromagnetic clusters, for which the FMR signal is associated with, and paramagnetic regions between clusters, giving rise to the PMR signal. Interestingly, it follows from the EPR data that the complex magnetic landscape formed by clusters in ferromagnetic Griffiths phases can exist both above and below the Curie point [42, 46–48]. It can be concluded that the data on electron paramagnetic resonance known from the literature are in good qualitative agreement with the model concepts underlying the Griffiths cluster model of the ferromagnetic phase.

4. The effect of impurity atoms and magnetic disorder on the physical properties of manganese monosilicide MnSi

4.1 The experimental situation before the discovery of the $Mn_{1-x}Rh_xSi$ system

In this section, we will consider classical experimental data concerning the effect of impurity atoms on the physical properties of manganese monosilicide. For this material, both manganese and silicon substitutions are possible. First, the most thoroughly studied situation arising from the replacement of manganese by iron or cobalt impurities in the substitutional solid solutions $Mn_{1-x}Fe_xSi$ and $Mn_{1-x}Co_xSi$ [49–55] will be analyzed. As long as the boundary compounds MnSi, FeSi, and CoSi possess the same B20 structure, the entire series of solid solutions with intermediate composition is possible in the range $0 \leqslant x \leqslant 1$. However, most studies have been performed for the compositions on the MnSi side. For example, the seminal work [49] reported the properties of single crystals with the cobalt and iron content of $x(\mathrm{Co}) \leqslant 0.04$ and $x(\mathrm{Fe}) \leqslant 0.19$. In [51, 52] the range of iron concentration in $Mn_{1-x}Fe_xSi$ was extended up to $x(\mathrm{Fe}) = 0.3$ and therefore this material will be the main object of our analysis.

It would be no exaggeration to say that manganese monosilicide and solid solutions based on it are popular objects of study in condensed matter physics, and the relevance of research has remained for half a century. This situation is associated with both nontrivial physical properties and with an ambiguous interpretation of the magnetic properties of this strongly correlated metal, developed in the literature. For $T < 29$ K, the incommensurate magnetic structure appears in MnSi, which, according to neutron studies, is a spiral with a period of 18 nm. Since the B20 structure does not have an inversion center, the appearance of the magnetic spiral is interpreted as a result of the simultaneous influence of the main ferromagnetic exchange J and the weaker Dzyaloshinskii–Moriya interaction D, allowed in this case by the symmetry of the crystal. In the simplest version, the spatial period of the spiral is $L \sim aJ/D$, which for $J \gg D$ significantly exceeds the lattice constant $a = 0.456$ m [50, 52, 53]. The first wave of interest in MnSi studies was associated with the appearance of Moriya's theory of itinerant magnetism [56], in which this material is considered as one of the main confirming examples. This approach was proposed to explain the paradox observed in some magnets, where the magnitude of the magnetic moment determined from the Curie–Weiss law for magnetic susceptibility in the paramagnetic phase is equal to units of the Bohr magneton per magnetic ion. But the saturated magnetization in the ferromagnetic phase in the limit $T \to 0$ turns out to be significantly less than this value, although one might intuitively expect all spins to align parallel (or almost parallel as in the helix of MnSi) and the saturation moment to coincide with the value found from $\chi(T)$. For example, for MnSi, the experimental data on susceptibility and LDA calculations give a magnetic moment of manganese of $(1.2-1.3)\mu_B$ [21, 57–60], and the saturated magnetization in the magnetically ordered phase is $\sim 0.3\mu_B/\mathrm{Mn}$ [21, 57–60].

Although MnSi is still classified as an itinerant magnet in some studies, electron paramagnetic resonance experiments [57–59] have shown that in this compound as well as in $Mn_{1-x}Fe_xSi$ solid solutions [61] the magnetic moment is localized on the manganese atoms. To explain the discrepancy between the magnitude of the localized magnetic moment and the saturation magnetization, a spin-polaron model, which takes into account the emergence of quasi-bound states linking the itinerant electrons and the magnetic moments of manganese, was proposed [21, 54, 59]. A detailed description of this model is given in Section 5. This approach not only explained the above-mentioned paradox underlying Moriya's theory, but also made it possible to describe for the first time the features of the field dependences of the magnetization in MnSi. From this point of view, the magnetic interactions in MnSi must be described within the Heisenberg paradigm, taking into account the interaction with charge carriers. It is obvious that in $Mn_{1-x}Fe_xSi$, the effects caused by magnetic disorder associated with the substitution of manganese by iron atoms, which in this compound can be considered nonmagnetic, can also be significant [57–59].

The second wave of interest in MnSi was caused by the discovery of the skyrmion lattice [62–64], the topological Hall effect [65], and quantum phase transitions [49, 51, 52, 66] in this material. The skyrmion lattice in MnSi arises in the so-called A-phase representing a narrow region on the $H-T$ magnetic phase diagram in the vicinity of the transition to the helical state [62–64], which can be identified by neutron scattering [62], Lorentz microscopy [63], and magnetotransport measurements [64]. The nontrivial spin structure of the A-phase leads to the emergence of the topological Hall effect [65].

The observation of quantum critical phenomena in MnSi is associated with both high-pressure experiments and the introduction of impurity atoms. It is known that the application of an external hydrostatic pressure of $p \sim 1.5$ GPa leads to a decrease in the transition temperature to the helical state to zero and the appearance of a quantum critical point [66]. Another method is the substitution of iron or cobalt for manganese, which also leads to suppression of the magnetic transition temperature [49, 51, 52, 55]. However, the physics associated with the mechanisms of property modification of MnSi by impurity atoms has remained in the background until recently. Below, we will show that this issue is no less interesting and fundamental than skyrmion physics, and, apparently, may prove important for the further development of the fundamental physics of magnetic phenomena.

The first detailed study of the physical properties (magnetic susceptibility, magnetization, AC magnetic susceptibility, heat capacity) of $Mn_{1-x}Fe_xSi$ and $Mn_{1-x}Co_xSi$ was performed in [49]. Based on extensive experimental data, it was shown that iron and cobalt impurities lead to a decrease in the temperature of the transition to the spiral phase with long-range magnetic order $T_{LRO}(x)$, and the quantum critical regime with $T_{LRO}(x)=0$ is achieved at $x(\mathrm{Co}) \sim 0.06$ or at $x(\mathrm{Fe}) \sim 0.15$ [49]. Analysis of the field dependences of magnetization in a magnetic field of up to 9 T at different temperatures using the Belov–Arrott method made it possible to find the temperature of ferromagnetic ordering $T_C(x)$, which turned out to be higher than $T_{LRO}(x)$ [49]. In addition to these temperatures, the heat capacity data in a magnetic field of up to 9 T showed that $Mn_{1-x}Fe_xSi$ and $Mn_{1-x}Co_xSi$ have another characteristic temperature $T_f(x)$ that exceeds $T_C(x)$ [49], and which can be associated with the magnetic fluctuations in the paramagnetic phase [53]. Thus, one of the main results of [49] is the hierarchy of characteristic temperatures $T_{LRO}(x) < T_C(x) < T_f(x)$ established in this work.

The next important step towards understanding the $T-x$ magnetic phase diagram was made in [50], where the small-angle polarized neutron scattering (SANS) data were compared with the features of the temperature dependence of the magnetic susceptibility in the $Mn_{1-x}Fe_xSi$ system. It was shown that the maximum and minimum in the temperature dependence of the derivative $d\chi/dT$ corresponds to a qualitative change in neutron scattering (Fig. 5). For example, for the minimum temperature T_f, the symmetric pattern at $T > T_f$ (Fig. 5, region 1) is replaced by a characteristic crescent-shaped scattering at $T < T_f$ (Fig. 5, regions 2 and 3). At temperature of the maximum T_{LRO}, a spiral phase appears, which is manifested by well-defined Bragg reflections (Fig. 5, region 5). Interestingly, the data in [50] made it possible to identify another characteristic temperature T^*, separating regions 2 and 3 in Fig. 5. In this case, it is proposed in [50] to consider the singularity of the second derivative $\partial^2\chi/\partial T^2$ as the boundary of the regions. In this case, the crescent-shaped pattern in the interval $T_{LRO} < T < T^*$ (Fig. 5, region 3) turns out to be more pronounced compared to the interval $T^* < T < T_f$ (Fig. 5, region 2), while maintaining the qualitative picture of neutron scattering. A more clear physical reason can also be indicated, which makes it possible to distinguish this boundary inside the range $T < T_f$ [54]. For this, one can use the data on the inverse lifetime of spin fluctuations Γ, obtained in [50] from the neutron spin echo data. It was found that at $T = T^*$ there

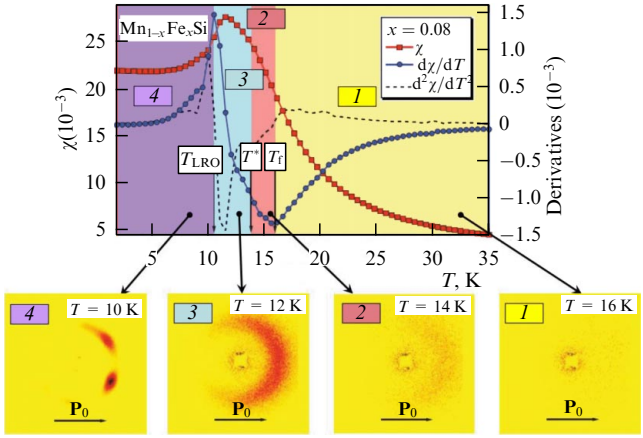

Figure 5. Correlation between the temperature dependences of the magnetic susceptibility χ, of the derivatives $d\chi/dT$, $d^2\chi/dT^2$ and the change in the small-angle scattering pattern of polarized neutrons for the $Mn_{1-x}Fe_xSi$ sample with $x = 0.08$ (according to [50]). (The details are in the text.)

is a maximum in the temperature dependence $\Gamma(T)$, indicating a change in the spin-fluctuation dynamics. Thus, the data [49, 50] show that in $Mn_{1-x}Fe_xSi$, in the vicinity of the transition to the spiral phase with long-range magnetic order, there is a complex fluctuation region.

The results of [50] were used in [51, 52] to construct the $T-x$ magnetic phase diagram of the $Mn_{1-x}Fe_xSi$ system, a feature of which is the presence of two quantum critical points: the first one $x^* \sim 0.11$ corresponds to the vanishing of the transition temperature into the spiral phase, $T_{LRO}(x^*) = 0$, and the second $x_c \sim 0.24$ — to the vanishing of the temperature defining the fluctuation region $T_f(x_c) = 0$. In [51], a model was also proposed for the quantitative description of the $T_f(x)$ dependence, which was later fully confirmed by data from the study of EPR and the anomalous Hall effect [52]. In this case, the region of the magnetic phase diagram $T < T_f$ was interpreted as the result of the 'freezing' of magnetic fluctuations and the formation of a phase with an intermediate magnetic order. An alternative approach to describing the fluctuation region was proposed in [53], where the boundaries between different regions were understood not as magnetic transitions, but as crossovers between temperature diapasons that differ in the nature of magnetic interactions.

The contradiction between the approaches [51, 52] and [53] was resolved within the concept of spin-fluctuation transitions [54]. A spin-fluctuation transition (SFT) is understood as an abrupt change in the characteristics of spin fluctuations (e.g., their amplitude or spatial orientation) in a magnet under the influence of control parameters (temperature or material composition), not directly related to the formation of phases with long-range magnetic order. For an experimentalist SFTs appear as clearly marked changes in the macroscopic characteristics occurring at a well-defined temperature, and from a theoretical point of view, in most cases, they go beyond the standard theory of phase transformations, for which it is typical to consider fluctuations as some phenomenon accompanying a magnetic transition. In a number of cases, SFTs can be considered as a magnetic analogy of phase transitions in liquid crystals. In particular, the transition from the isotropic liquid phase to the nematic phase is accompanied by a change in the X-ray scattering

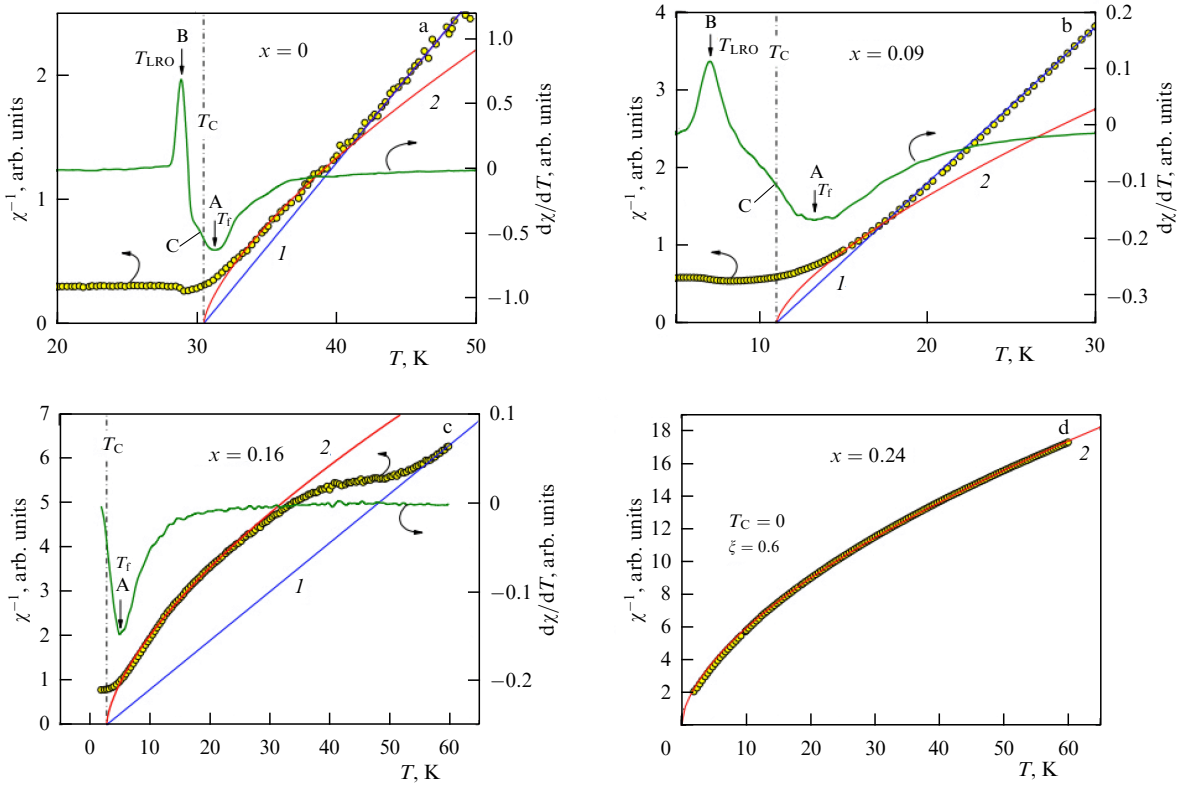

Figure 6. Temperature dependences of the inverse magnetic susceptibility χ^{-1} and the derivative $d\chi/dT$ for $Mn_{1-x}Fe_xSi$ samples of different compositions: a $x = 0$, (b) $x = 0.09$, (c) $x = 0.16$, (d) $x = 0.24$. In panels a–d, the solid lines denote the asymptotic behavior of the magnetic susceptibility in the cluster model of a disordered ferromagnet: *1* — the Curie–Weiss law (Eqn (10)); *2* — the power dependence (Eqn (11)). Letters A, B, and C mark various features of the temperature dependence of $d\chi/dT$ (see text). (The experimental data are taken from [51].)

pattern, identical to that shown in Fig. 5 for magnetic scattering [67]. In the case of a magnet, the rod-shaped molecules in a liquid crystal are emulated by anisotropic spin fluctuations, and the transition from the paramagnetic phase to the spin nematic phase corresponds to a transition from isotropic fluctuations to anisotropic ones without establishing any long-range magnetic order [68]. It is expected that the SFT of this type occurs in $Mn_{1-x}Fe_xSi$ at $T = T_f$ [54].

The occurrence of a quantum critical regime caused by the Griffiths phase in $Mn_{1-x}Fe_xSi$ was first discovered in [51]. According to this work, in the region of compositions $x > x_c$, the magnetic disorder becomes so strong that the magnetic subsystem decay into separate clusters. In this case, a characteristic power-law dependence of the magnetic susceptibility $\chi \sim 1/T^{\xi}$ with the exponent $\xi = 0.5-0.6$ is observed in the experiment [51, 52]. However, the question of the existence of the Griffiths phase in the region $x < x_c$ was not considered in [51, 52], despite the fact that a decrease in T_{LRO} with x can be a consequence of the magnetic disorder influence. This circumstance was brought to attention in a recent study [55], in which low-temperature Griffiths-type anomalies of the magnetic properties were discovered in $Mn_{1-x}Fe_xSi$ in the concentration range $x < x_c$. In addition, in [55] an attempt was made to interpret the magnetic phase diagram within the framework of the scenario previously used to describe quantum critical phenomena in the $Co_{1+x}Sn$ and $Ni_{1-x}V_x$ systems [20, 36, 37], which does not take into account the presence of a second quantum critical point at $x = x_c$.

In view of the results obtained in [55], it is interesting to consider the existence of the Griffiths phase in the $Mn_{1-x}Fe_xSi$ system in more detail. For this purpose, we will use the theoretical model described in Section 2, with which we will analyze the experimental data from [51]. Typical results for the $\chi^{-1}(T)$ dependences are shown in Fig. 6, where curves *1* correspond to the Curie–Weiss law (10), and curves *2* to the Griffiths power-law asymptotics (11) with $T_C \neq 0$ (Fig. 6a–c) and with $T_C = 0$ (Fig. 6d). It is evident that a simple model taking into account only ferromagnetic interactions describes the experimental data well, which is apparently due to the small magnitude of the Dzyaloshinskii–Moriya interaction compared to the main ferromagnetic exchange. For small clusters, having a size smaller than or comparable to the period of the magnetic spiral $L \gg a$, the system can be approximately considered as ferromagnetic and, therefore, for the Griffiths phase with nanosized magnetic clusters, reasonable agreement with experiment should be expected (see Fig. 6).

A comparison with the temperature dependence of $d\chi/dT$ shows that the temperature T_f of the minimum A, corresponding to the spin-fluctuation transition, is always higher than the Curie temperature T_C, which in turn satisfies the condition $T_C > T_{LRO}$, where T_{LRO} is determined by the temperature of the maximum B (Fig. 6a–c). Qualitatively, this result corresponds to the analysis performed in [49], when the temperature associated with ferromagnetism lies between T_f and T_{LRO}. However, in our case, this result was obtained for the Griffiths ferromagnetic phase model and does not use an analysis of magnetization in Belov–Arrott coordinates as in [49]. Note that the use of Belov–Arrott or Arrott–Noack coordinates [68] is justified if the standard equation of state for a ferromagnet is valid [22] that, however, is not applicable

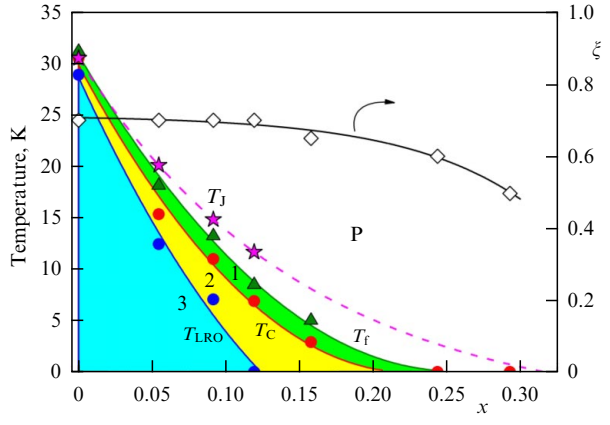

Figure 7. Magnetic $T-x$ phase diagram of $Mn_{1-x}Fe_xSi$ and temperature dependence of the exponent ξ, obtained from the analysis of magnetic susceptibility data using the disordered cluster ferromagnet model (the details are in the text).

to the Griffiths systems [1, 2, 5, 6]. Therefore, the phenomenological approach we use to find T_C is more consistent and provides a more accurate estimate of T_C compared to work [49]. It is interesting that for compositions in the interval $x < x^*$, when $T_{LRO} \neq 0$, an additional feature C is observed on the $d\chi/dT = f(T)$ curve (see Fig. 6), the position of which on the temperature scale coincides with the change in the lifetime of spin fluctuations and in the small-angle neutron scattering pattern discovered in work [50]. Thus, within the limits of experimental accuracy, the condition $T_C \approx T^*$ is satisfied (Figs. 5, 6).

The found dependences $T_{LRO}(x)$, $T_C(x)$ and $T_f(x)$ are shown in Fig. 7, where the dots represent the result of the magnetic susceptibility processing, and the lines reflect the qualitative behavior of the concentration dependences of the characteristic temperatures with a change in the iron concentration in the $Mn_{1-x}Fe_xSi$ solid solution. An accurate description of the SFT temperature $T_f(x)$ with the help of the corresponding quantitative model is given in [51, 52, 54].

The data in Figs. 6 and 7 allows us to draw several important conclusions. First, the transition from the paramagnetic phase to the helical phase with long-range magnetic order occurs in several stages. With decreasing temperature, a spin-fluctuation transition to the spin-nematic phase (region 1 in Fig. 7) first occurs at $T = T_f$, and then the ferromagnetic Griffiths phase is formed at $T = T_C$ (region 2 in Fig. 7). Since the cluster model describes the transition at T_C well, it is necessary to assume the existence of magnetic clusters both at $T_f > T > T_C$ and at $T < T_C$. Since the SFT occurs at $T = T_f$, the decay into clusters may fluctuate in time and this process must be slow enough for correlations to be established between the clusters and, as a result, a quasi-stationary distribution function of local fields, given by formula (2), to emerge. The concentration dependence of the exponent $\xi(x)$ found from the approximation of the $\chi^{-1}(T)$ curve section by Eqn (11) turns out to be quite weak, and in the region $x < 0.3$ this parameter takes values from the range 0.5–0.7 (see Fig. 7), which indicates a smooth and not very pronounced evolution of the local magnetic field distribution function. Note that at $T = T_C$ the magnetic fluctuations should slow down even more, and therefore we assume that the temperature T^*, at which the disordered crescent-shaped magnetic scattering becomes sharper due to a change in spin dynamics (see Fig. 5, [50]), coincides with T_C following from the cluster model of the Griffiths phase. This qualitatively considered scenario of the Griffiths phase formation can be regarded as a 'freezing' of magnetic fluctuations in the vicinity of T_{LRO}.

Secondly, as long as the formation of the phase with long-range magnetic order (region 3 in Fig. 7) with decreasing temperature is preceded by the emergence of the Griffiths phase, it cannot be ruled out that in $Mn_{1-x}Fe_xSi$ magnetic disorder plays such a significant role that the transition at T_{LRO} to the helical phase not only is caused by the combined influence of ferromagnetic exchange and the Dzyaloshinskii–Moriya interaction, but is also associated with percolation due to the merging of individual clusters. In the absence of the Dzyaloshinskii–Moriya interaction, such a percolation phase would be a conventional ferromagnet; however, taking this term into account in the spin Hamiltonian will create a resulting helical magnetic structure. In this case, magnetic fluctuations at $T > T_{LRO}$ in a certain fairly narrow temperature range will also have a helical rather than purely ferromagnetic character, which is observed experimentally [50, 53].

Thirdly, the fundamentally important fact is that at $x = 0.16$ the temperature of the ferromagnetic transition to the Griffiths phase T_C for $Mn_{1-x}Fe_xSi$ is nonzero (see Fig. 6c). This result allows one to take a new look at the estimate of the magnetic interaction in this system, performed in [69, 70]. In [70], an analysis of neutron scattering data made it possible to find the concentration dependence of the exchange energy $J(x)$ in the region $x < 0.1$, from the extrapolation of which it follows that the ferromagnetic exchange should vanish at $x \sim 0.15$. In [69], from the data on the Hall effect for compositions with $x < 0.3$ and the $J(x)$ dependence for $x < 0.1$, the RKKY function was found for compositions with different iron concentrations. The calculation confirmed that the exchange integral between the nearest ferromagnetic neighbors in the MnSi structure vanishes at $x \sim 0.15$ and, with a further increase in the iron concentration, changes sign to the opposite, corresponding to the antiferromagnetic interaction [69]. At the same time, the exchange between the next-to-nearest neighbors always remained of the antiferromagnetic type and depended weakly on the value of x [69]. If these results are correct, then for the sample with $x = 0.16$, the antiferromagnetic interaction rather than the ferromagnetic one should dominate, and the magnetic susceptibility for this composition cannot be described by the Griffiths cluster ferromagnetic phase model. This statement clearly contradicts the experiment, which demonstrates good agreement with our theory (see Fig. 6c).

The discrepancy between the analysis performed in the present work and the results of [69, 70] may be due to several reasons. First of all, attention should be paid to the difficulty of separating the electron and hole contributions to the Hall coefficient, which is necessary for the correct determination of the Fermi momenta of electrons and holes, as well as to the rather crude spherically symmetric approximation used in [69] to calculate the RKKY interaction between magnetic manganese ions. In addition, it should be taken into account that when constructing the $J(x)$ dependence in [70], nominal values of the iron concentration in the solid solution were used, which differed slightly from the actual values measured for specific compositions. This circumstance could not but affect the result of the extrapolation of the $J(x)$ data.

In this study, we corrected the concentration dependence $J(x)$ taking into account the actual iron concentration and

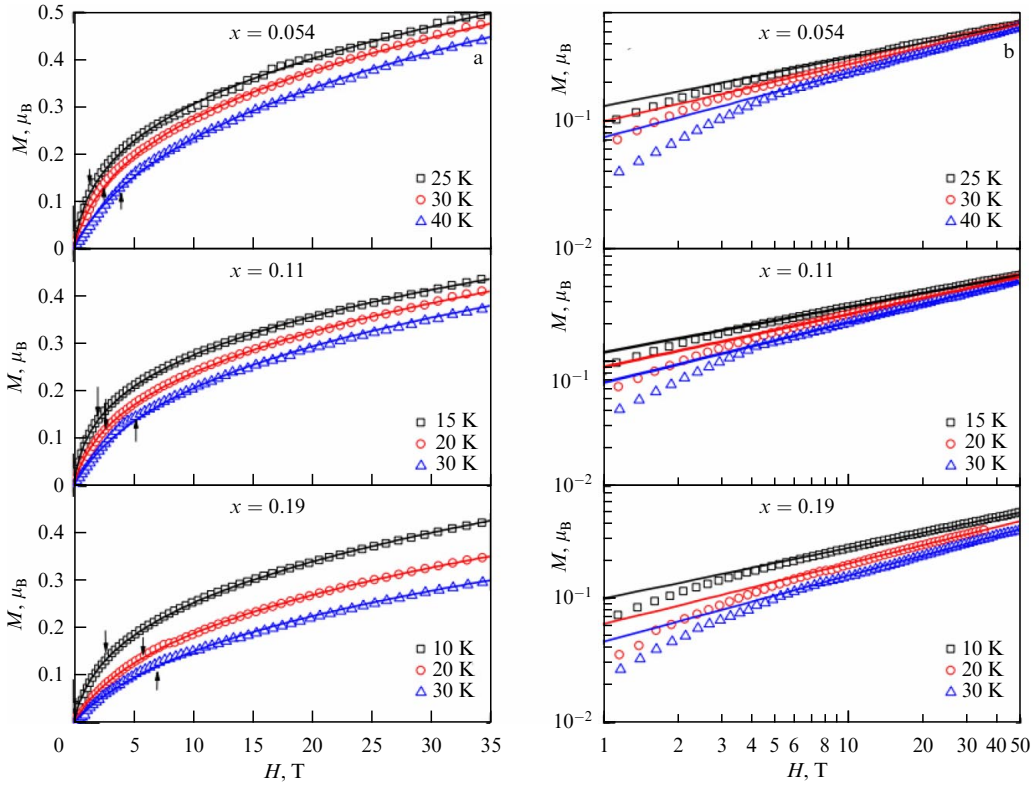

Figure 8. Power-law field dependences of the magnetization in $Mn_{1-x}Fe_xSi$ samples of different compositions in a magnetic field of up to 50 T. (a) The arrows indicate the magnetic field H_c, above which the power-law dependence $M \sim H^{\alpha}$ is observed. (b) The $M(H)$ data are presented in double logarithmic coordinates. (From [71].)

constructed a model temperature dependence $T_J(x) = T_C(0)J(x)/J(0)$, which could describe the ferromagnetic transition if the only reason for the change in T_C were a change in J (see Fig. 7). It is evident that $T_J(x)$ yields temperatures significantly higher than the experimentally observed T_C values, with the mismatch increasing with x. This behavior is entirely consistent with the physics of the Griffiths phase, for which an additional decrease in T_C should be observed due to magnetic disorder, which increases with iron content in the solid solution. In addition, the refined concentration dependence shows that the exchange integral, if it vanishes, does so only in the vicinity of $x \sim 0.3$ (see Fig. 7), confirming the validity of the experimental data analysis performed using the cluster model of the Griffiths ferromagnetic phase.

In light of the study of Griffiths physics in the $Mn_{1-x}Fe_xSi$ system, the work [71] is of considerable interest where the field dependences of magnetization $M(H)$ were investigated in the range $H < 50$ T. It was found that the excess of the critical value $H_c \sim 1.5-7$ T, depending on the temperature and composition of the sample, leads to the magnetization in the paramagnetic phase following an empirical power law

$$M(H, T) = A(T)H^{\alpha(T)} \tag{15}$$

with an exponent $\alpha \sim 0.33-0.5$, which is fulfilled up to the maximum field of ~ 50 T (Fig. 8). This unusual behavior was interpreted as the occurrence of a magnetic field-induced Griffiths phase [71]. It was assumed that in the region $H > H_c$, the magnetic field suppresses magnetic fluctuations and stabilizes magnetic inhomogeneities associated with them, thus leading to the appearance of some effective disordered cluster structure [71]. If this assumption is correct, then, according to the Griffiths phase model (Section 2), a strong magnetic field in $Mn_{1-x}Fe_xSi$ creates a cluster ferromagnetic phase with dispersion of local fields. In such a situation, as noted above, the parameter $A(T) \sim M_0(T)$ can be used to estimate the temperature dependence of the order parameter [16, 18]. The temperature dependences of $A(T)$ from [71] are shown in Fig. 9. Although the experimental data are not very detailed, it is clear that the coefficient $A(T)$ decreases with increasing temperature, and extrapolation of the $A(T)$ temperature dependence to the value $A = 0$ gives an estimate of the Curie temperature $\sim 46-60$ K in the field-induced ferromagnetic Griffiths phase (see Fig. 9).

However, in the considered model, the combination $H_m^{1-\xi}$ can contribute to the temperature dependence of $A(T)$ (Eqn (12)). It follows from the data in [71] that the temperature dependence of the exponent $\xi(T) = 1 - \alpha(T)$ does not exhibit critical behavior; therefore, only the parameter H_m can make an additional contribution to the critical temperature dependence of $A(T)$. Formally, this parameter is introduced in order to satisfy the normalization condition (2a), as long as the corresponding integral diverges at the upper limit and, in principle, may be independent of temperature. If we assume a significant temperature dependence of the cutoff field, which has a physical meaning, then it is necessary to assume that the value of H_m specifies the range of actual local fields in which the power-law dependence (12) will be satisfied. Local fields, in turn, are associated with the magnetization of clusters in the Griffiths phase, which decreases at $T \to T_C$ according to Eqn (13). As a result, the dispersion of local fields will decrease rather than increase.

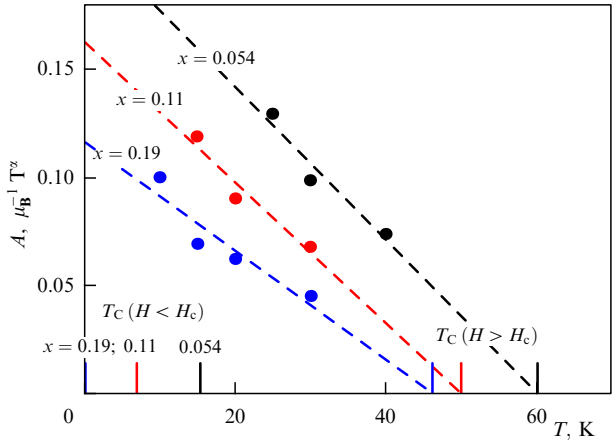

Figure 9. Temperature dependences of the order parameter (coefficient A in Eqn (15)) and comparison of the Curie temperatures in the low-field magnetic phase ($H < H_c$) and in the magnetic field-induced Griffiths phase ($H > H_c$).

Therefore, as the Curie temperature approaches the region of existence of the FM phase, within the framework of the considered 'physical' interpretation, the parameter H_m should decrease, which should lead to an increase in the value of $A(T \to T_C)$. This behavior contradicts the experiment (see Fig. 9). Thus, a comparison of the model with the experimental data shows that the main contribution to the temperature dependence of $A(T)$ comes from the temperature dependence of the order parameter, rather than from H_m or ξ. However, a slight overestimation of the Curie temperature estimated from $A(T)$ cannot be ruled out.

Nevertheless, it can be concluded from Fig. 9 that in the magnetic field-induced Griffiths phase, the T_C value significantly exceeds the Curie temperature for the Griffiths phase, which arises from the 'freezing' of magnetic fluctuations (see Fig. 7). For example, in the sample with $x = 0.054$, the characteristic T_C temperature increases from ~ 15 K to ~ 60 K, and for the composition with $x = 0.11$, from ~ 7 K to ~ 50 K, that is, the Curie temperature increases by a factor of 4–7. For the sample with $x = 0.19$, the effect of the magnetic field is even more significant: whereas in a weak magnetic field almost complete suppression of the magnetic transition temperature $T_C \approx 0$ should be achieved with experimental accuracy (see Fig. 7), in the strong magnetic field a Curie temperature of $T_C \sim 46$ K arises (see Fig. 9). Thus, the experiment demonstrates that the generally accepted universal decrease in the magnetic transition temperature within the Griffiths scenario is sometimes violated, and the emergence of the Griffiths phase can be accompanied by a significant increase in the Curie temperature. This effect will be discussed in more detail in the next section using the example of the new $Mn_{1-x}Rh_xSi$ system.

In conclusion of this section, we will consider the effect of the atoms substituting silicon in manganese monosilicide [72]. In this case, there are no data in the literature that may allow one to analyze the structure of the fluctuation region, and only information available is the magnetic transition temperature, which, to a first approximation, can be considered as the Curie temperature corresponding to the strongest type of magnetic interaction in MnSi [72]. A study of the magnetic properties of $MnSi_{1-x}Al_x$ ($x < 0.04$), $MnSi_{1-x}Ga_x$ ($x < 0.01$) and $MnSi_{1-x}Ge_x$ ($x < 0.1$) single crystals showed that, in this concentration range, samples with impurities exhibit an increase in T_C up to ~ 40 K. The substitution by aluminum, gallium, and germanium atoms of the silicon atoms leads to an increase in the lattice constant a, so the effect of an increase in the magnetic transition temperature is described as the effect of 'negative chemical pressure' [72], since both T_C and a decrease under pressure [66]. Obviously, impurities generally induce the emergence of a random deformation field, and in the case of 'negative chemical pressure,' we mean the average value of the crystal lattice parameters depending on the concentration of the impurity atom. An analysis of the possible influence of 'negative chemical pressure' on the ferromagnetic transition temperature in the Griffiths phase will be carried out in Section 5.4. Note that, as expected, for an iron impurity replacing manganese, the lattice constant of the $Mn_{1-x}Fe_xSi$ compound decreases [72]. In this case, one can obviously discuss the 'positive chemical pressure.'

4.2 New magnets with the B20 structure: MnSi–RhSi substitutional solid solutions

The first report on the physical properties of MnSi-based solid solutions in which manganese atoms are replaced by rhodium atoms was published in [15]. As in the case of $Mn_{1-x}Fe_xSi$ and $Mn_{1-x}Co_xSi$, there is a boundary compound RhSi, which has the same noncentrosymmetric crystal structure B20 as MnSi. Therefore, the synthesis of $Mn_{1-x}Rh_xSi$ substitutional solid solutions is possible in a wide range of compositions $0 \leqslant x \leqslant 1$. In [15], the polycrystalline $Mn_{1-x}Rh_xSi$ samples were synthesized by a high-pressure technique [73]. The initial sample of high-purity manganese (99.9%), rhodium (99.97%) and silicon (99.999%) was placed in an insulating container made of single-crystal NaCl and then subjected to the simultaneous action of a pressure of 8 GPa and a high temperature of 1500–1700 K in a toroid-type chamber. X-ray diffraction analysis confirmed that in the composition range $0 \leqslant x \leqslant 1$, the samples crystallize in the B20 structure with a lattice constant increasing with the growing rhodium content and, consequently, a case of 'negative chemical pressure' is realized in these substitutional solid solutions (Fig. 10). This circumstance radically distinguishes the influence of rhodium atoms from the influence of iron or cobalt atoms, for which the lattice constant decreases with respect to MnSi [49, 72]. In this case, deviations from Vegard's law are observed, and the

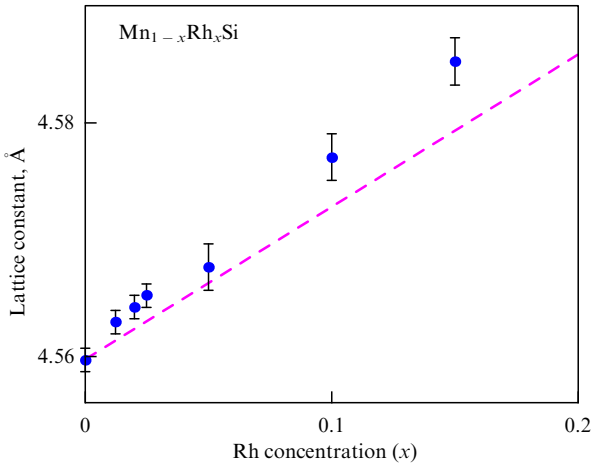

Figure 10. Dependence of the lattice constant of $Mn_{1-x}Rh_xSi$ substitutional solid solutions on the rhodium concentration. The dashed line corresponds to Vegard's law. (From [15].)

dependence of the lattice constant on the concentration is nonlinear (see Fig. 10). The homogeneity and stoichiometry of the samples were monitored using scanning electron microscopy and X-ray microanalysis. Relative deviations of the composition from the nominal chemical formula $Mn_{1-x}Rh_xSi$ did not exceed 1% and, from this point of view, the composition of the samples was at the same quality level as in the single crystals of the $Mn_{1-x}Rh_xSi$ system studied previously [51, 52, 61, 69, 70, 71].

The study of the magnetic structure of $Mn_{1-x}Rh_xSi$ samples performed by the neutron scattering method showed that the Dzyaloshinskii–Moriya interaction exists up to compositions with $x \sim 0.13$, and for samples with a rhodium content of $x \leqslant 0.02$, not only a spiral phase can be observed, but also the formation of an A-phase occurs, in which a skyrmion lattice exists [15]. Moreover, the temperature range of the existence of the A-phase in $Mn_{1-x}Rh_xSi$ has significantly expanded in relation to the original MnSi [15]. Interesting information about the magnetic state of manganese atoms was obtained in a study of nuclear magnetic resonance (NMR) spectra in zero external magnetic field [15]. In this case, resonant absorption is due to the presence of local magnetic fields in the sample, which, in turn, depend on the magnitude of the magnetic moment of the atoms in the crystalline structure of the material [74].

Experimental NMR spectra of $Mn_{1-x}Rh_xSi$ on the ^{55}Mn nucleus for zero external magnetic field at liquid-helium temperatures are shown in Fig. 11. At $x \leqslant 0.02$, a multimodal line shape characteristic of the helical phase is observed, peaking at ~ 48 MHz. In the transition region of $x = 0.025$, the low-frequency signal of the helical phase coexists with two new structureless absorption lines at ~ 185 MHz and ~ 315 MHz. Increasing the rhodium concentration to $x = 0.05$ results in the disappearance of the resonance associated with the helical phase, and only new absorption features remain in the NMR spectra. For the sample with $x = 0.15$, in the frequency range where the spiral phase response was previously observed, a broad spectrum with weakly expressed resonant features is seen, while the 'double-humped' structure of the spectra characteristic of high frequencies is preserved, but the positions of the maxima shift to frequencies of ~ 200 MHz and ~ 325 MHz (see Fig. 11). Interestingly, the amplitude of the line with the maximum frequency increases with increasing rhodium concentration, and for $x \sim 0.15$, this feature in the spectra turns out to be the main one.

The ratio of the frequencies of the maxima in the NMR spectra for zero external magnetic field 48 MHz:185–200 MHz:315–325 MHz can be used to estimate the magnitude of localized magnetic moments (LMMs) in $Mn_{1-x}Rh_xSi$ samples [74]. In the general case, there will be three such LMMs, and their relative values will be scaled as characteristic frequencies, $\mu_1{:}\mu_2{:}\mu_3 = 1{:}(3.85-4.16){:}(6.56-6.77)$. If we accept that the smallest value of μ_1 is associated with the reduced LMM of manganese in MnSi $\sim 0.3\mu_B$, then $Mn_{1-x}Rh_xSi$ may also have magnetic moments of $\mu_2 \sim (1.15-1.25)\mu_B$ and $\mu_3 \sim (1.96-2.03)\mu_B$. In this case, doping with rhodium suppresses magnetic centers with $\mu_1 \sim 0.3\mu_B$ and induces the appearance of LMMs with $\mu_2 \sim 1.2\mu_B$ and $\mu_3 \sim 2\mu_B$. In [15], this effect was interpreted as a transition

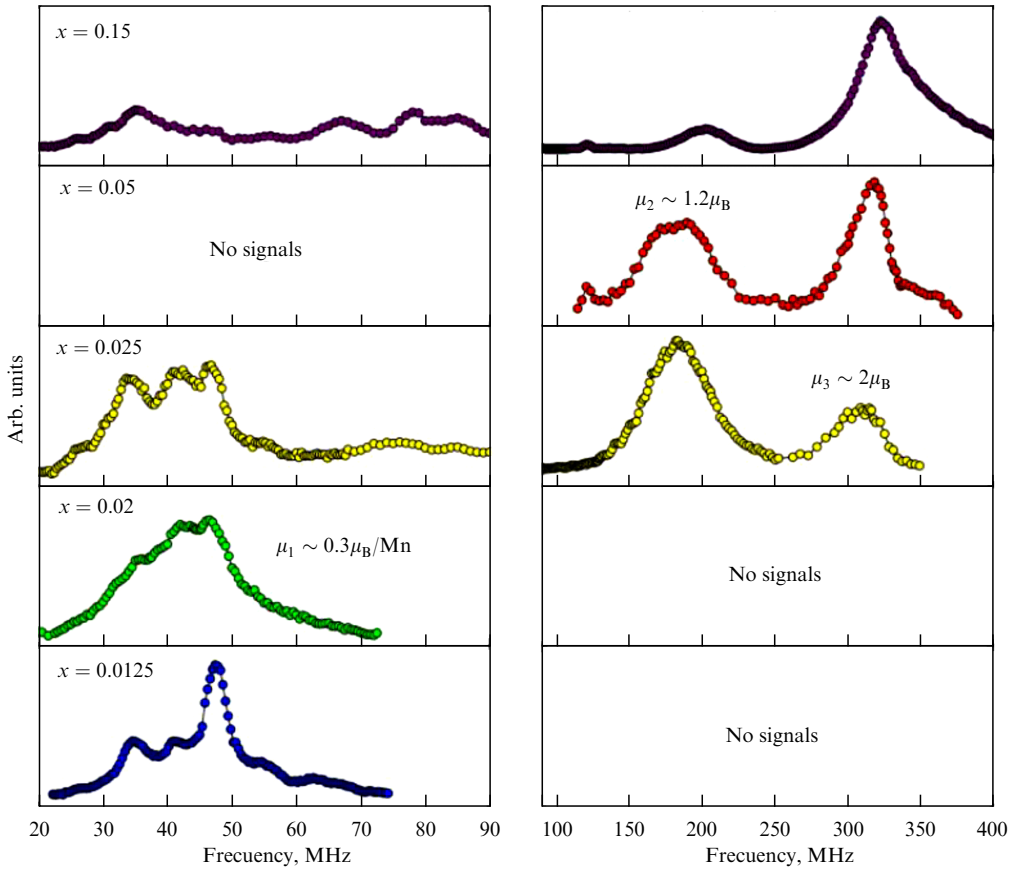

Figure 11. Experimental NMR spectra on the ^{55}Mn nucleus in zero external magnetic field at helium temperatures for $Mn_{1-x}Rh_xSi$ samples of different compositions. (From [15].)

between different states of the manganese ion: low-spin and high-spin. However, in this case, it is necessary to explain not one, but two high-spin values of the LMM, which, of course, presents a certain difficulty. The performed DFT calculations led the authors of [15] to the conclusion that when introducing rhodium atoms into a manganese monosilicide matrix, it is necessary to take into account the variation in the local environment, which results in a change in the spin state of the Mn atoms. According to [15], this effect originates from of the appearance of a group of manganese atoms with small moments of several tenths of μ_B and another group with moments of about $1.0\mu_B$, as well as some individual Mn atoms with a maximum moment of about $1.8\mu_B$ [15]. In order to obtain these values, although close to the experimental ones, but slightly different from them, it is necessary to postulate additionally both certain violations of the stoichiometric composition and the existence of some specially selected intermetallic phases, the presence of which in the samples, however, is not confirmed by the structural studies data [15]. In addition, it is necessary to take into account the appearance of a magnetic moment on the rhodium atom [15]. Note that within the framework of this approach, it is difficult to explain the coexistence of all three signals from μ_1, μ_2 and μ_3 in the NMR spectrum of the sample with a low rhodium concentration $x = 0.025$ (see Fig. 11). Indeed, in this case, the rhodium content is low, and it is difficult to imagine a situation in which different types of local environment with a comparable concentration of manganese atoms would be present in these special configurations. Note that the presence of a complex absorption pattern in the frequency range of 20–100 MHz for the sample with $x = 0.15$ can be explained by the dispersion of the local magnetic fields, which may indicate the formation of a cluster ferromagnetic phase of the Griffiths type. This possibility was not considered in [15].

It should be noted that the modeling performed in [15] does not take into account the spin-polaron effects determining the magnetism of manganese monosilicide, which were previously established experimentally [54, 57–59, 71] and confirmed using a theoretical description [21]. As we will see further in Section 5, this approach allows one to provide an alternative, and apparently simpler, explanation for the observed evolution of the NMR spectra.

4.3 The Griffiths phase and ferromagnetism in $Mn_{1-x}Rh_xSi$

The first report that the substitution of manganese by rhodium in the $Mn_{1-x}Rh_xSi$ solid solution for compositions $x \leqslant 0.15$ leads to a strong increase in the Curie temperature to temperatures of $\sim 180-250$ K, which significantly exceed the magnetic transition temperature of ~ 29 K in pure MnSi, was published in [15]. This result is illustrated in Fig. 12, where the temperature dependence of the inverse magnetic susceptibility for $Mn_{1-x}Rh_xSi$ sample with $x = 0.15$ is shown. It is evident that the experimental data (Fig. 12, curve *1*) are in good agreement with the Griffiths cluster model of the ferromagnetic phase when choosing the parameters $T_C = 248$ K and $\xi = 0.7$ (Fig. 12, curves *2*, *3*). The intersection point $T_{cr} \sim 268$ K of the Curie–Weiss asymptotic (curve *2*) and the power-law dependence (11) (curve *3*) allows one to estimate the field H_m as ~ 30 T. Thus, it can be expected that in a wide range of magnetic fields $H < H_m$ in $Mn_{1-x}Rh_xSi$ for $T < T_C$ an anomalous power-law field dependences of the magnetization may be observed.

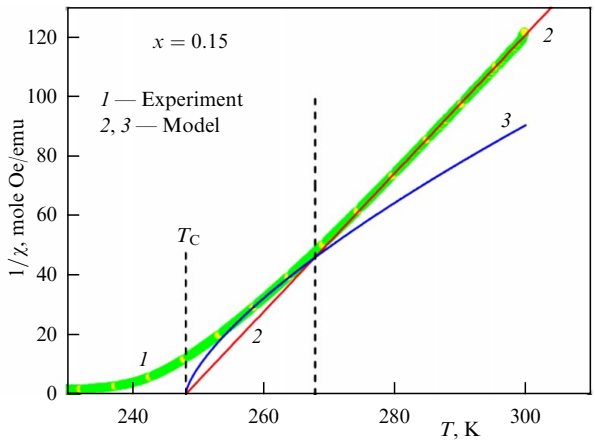

Figure 12. Temperature dependence of the inverse magnetic susceptibility for the $Mn_{1-x}Rh_xSi$ sample with $x = 0.15$ (curve *1*) and the asymptotic behavior of the magnetic susceptibility in the Griffiths cluster model of the ferromagnetic phase: *2* — Curie–Weiss law (Eqn (10)), *3* — power dependence (Eqn (11)). (Experimental data are taken from [15].)

The study carried out in [16] fully confirmed this assumption. Examples of experimental curves $M(H)$ for samples with $x = 0.15$ and $x = 0.8$ in the range $H \leqslant 9$ T are shown in Fig. 13a, b. Comparing the empirical and theoretical dependences (15) and (12) it is easy to see that in the cluster model of the Griffiths ferromagnetic phase, $\alpha = 1 - \xi$. Therefore, for comparison with the theory, it is convenient to represent the isotherms of the experimental field dependences of magnetization in the form

$$\frac{H}{M} = f(H) = \frac{H^{\xi(T)}}{A(T)}\,. \tag{16}$$

It is evident from Fig. 13 that Eqn (16) describes the experimental data well (panels c, d). Using the coordinates $H/M = f(H)$ immediately makes the absence of a linear response with respect to the magnetic field obvious, which can be described using the field-independent magnetic susceptibility, $M = \chi H$, as long as in this case the ratio H/M in the limit $H \to 0$ should reach a finite value $H/M = 1/\chi$. This behavior is inconsistent with the experiment, and in the case of $Mn_{1-x}Rh_xSi$, in accordance with (16), the ratio H/M tends to zero in the limit $H \to 0$ (Fig. 13c, d). Note that, as established in [16], for $Mn_{1-x}Rh_xSi$ in the region of compositions with $x \geqslant 0.1$, the magnetization M follows a power-law dependence on the magnetic field H with an exponent less than unity over a wide temperature range, where the temperature variation exceeds two orders of magnitude.

Approximation of the curves $H/M = f(H)$ allows us to find the exponent ξ and plotting the experimental data in rectifying coordinates $H/M = f(H^{\xi})$ (Fig. 14). The power-law dependence (16) describes the experimental $M(H)$ data well in a wide temperature range (Fig. 14a, b) with the exception of a small region in the vicinity of the origin of coordinates $H^{\xi} \leqslant 0.3\ \mathrm{T}^{\xi}$ for some curves, where a small hysteresis is observed in the field dependences of magnetization. The exponents $\xi(T)$ calculated from the approximation of the experimental data for samples with $x = 0.15$, $x = 0.4$ and $x = 0.8$ are shown in Fig. 14c. The same data were used to construct rectifying coordinates in the panels a, b of Fig. 14. It is visible that for $Mn_{1-x}Rh_xSi$ the value of the exponent ξ is ~ 0.7 and is weakly dependent on temperature.

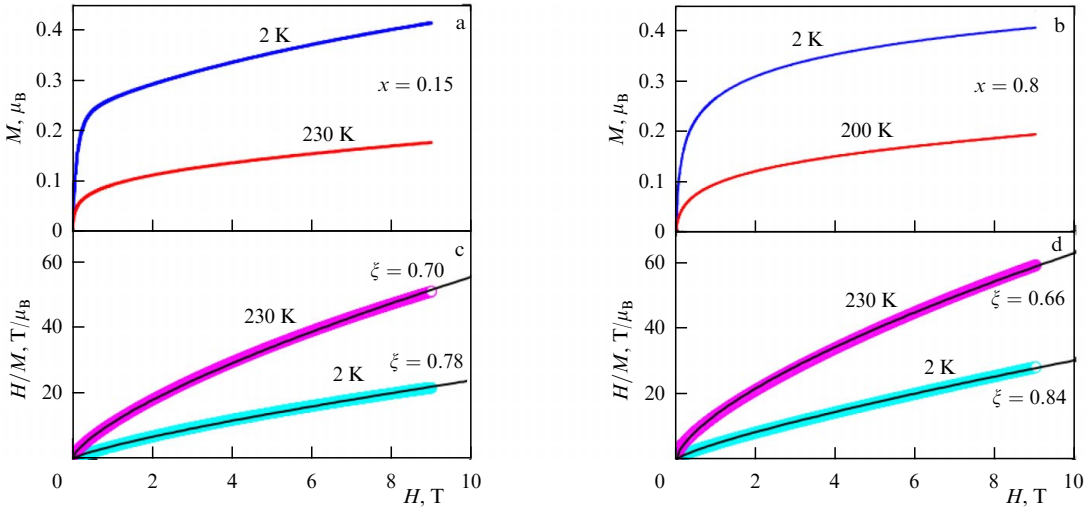

Figure 13. Examples of the dependence of magnetization M on the magnetic field H for $Mn_{1-x}Rh_xSi$ samples with $x = 0.15$ and $x = 0.8$ (panels a-b) and the $M(H)$ data re-plotted in coordinates $H/M = f(H)$ (panels c, d). Solid lines in the panels c and d are approximations of the experimental data using Eqn (16). (From [16].)

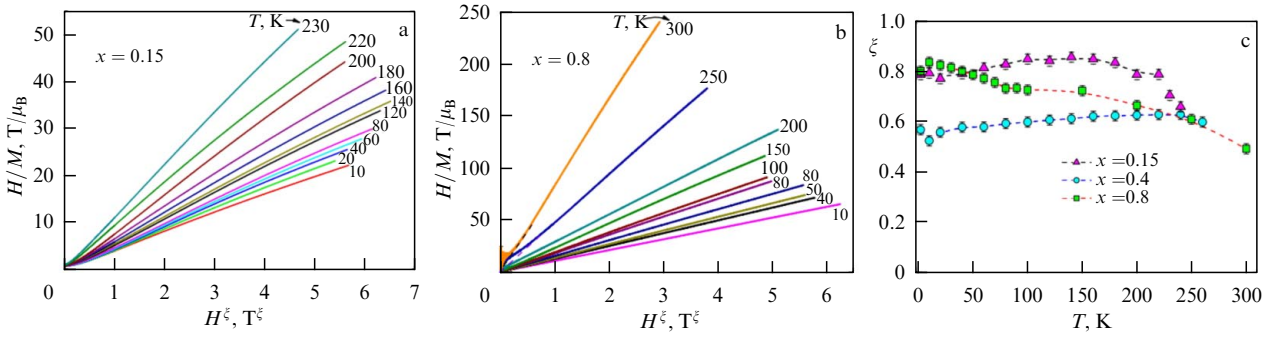

Figure 14. Field dependences of magnetization for $Mn_{1-x}Rh_xSi$ samples with $x = 0.15$ and $x = 0.8$ in rectifying coordinates $H/M = f(H^{\xi})$ (panels a, b) and temperature dependence of the exponent $\xi(T)$ for the samples with $x = 0.15$, $x = 0.4$ and $x = 0.8$. Numbers near curves in panels a, b correspond to the absolute temperature values. (From [16].)

As was shown in [16], the same arguments are applicable to $Mn_{1-x}Rh_xSi$ samples as in the case of the analysis of power-law dependences in the $Mn_{1-x}Fe_xSi$ system (Section 4.1) and the temperature dependence of the coefficient A in Eqn (16) can be used to estimate the temperature dependence of the order parameter $A(T) \sim M_0(T) \sim (T_C - T)^{\beta}$: see expressions (12) and (13). This statement is valid for the samples with a rhodium content of $x \geqslant 0.1$ [16]. Interestingly, for the sample with $x = 0.05$, a noticeably different behavior is observed [75]. In this case, the power-law field dependence of the magnetization coexists with the saturating contribution M_{sat}, and for $T < T_C$ the saturating contribution dominates. This situation is similar to the case of $Ni_{1-x}V_x$ [37] (see Section 3). The experimental data obtained in [75] show that for the sample with $x = 0.05$, it is the temperature dependence $M_{sat}(T)$ that has the form characteristic of the temperature dependence of the order parameter.

This result can be easily explained qualitatively within the framework of our Griffiths cluster model of the ferromagnetic phase, taking into account that magnetic disorder increases with rhodium content in the samples. As shown in Section 2, the clusters themselves behave like ordinary para- and ferromagnets with some saturated magnetization M_0. The anomalous magnetic response of the cluster system arises due to strong disorder caused by the dispersion of local magnetic fields. If the disorder is not too strong, the clustering of the magnetic system will be weakly expressed. As a result, the specific power-law contribution to $M(H)$ will not dominate and will coexist with the usual saturating contribution with $M_{sat}(T) \sim M_0(T)$. Therefore, at weak disorder, it is the saturating contribution $M_{sat}(T)$ at $T < T_C$ that provides information about the order parameter.

The experimental data on the temperature dependences of the order parameter found in [16, 75] are summarized in Fig. 15a. Approximation of $M_{sat}(T)$ for the sample with $x = 0.05$ and $M_0(T)$ for the samples with $x \geqslant 0.1$ using the critical dependence (13) in the vicinity of the magnetic transition temperature (solid lines in Fig. 15a) made it possible to find the Curie temperature and the critical index β. It is evident that the Curie temperature increases with increasing rhodium content from $T_C \approx 200$ K ($x = 0.05$) to $T_C \approx 350$ K ($x = 0.8$). Therefore, $Mn_{1-x}Rh_xSi$ exhibits the effect of a giant increase in the ferromagnetic transition temperature by a factor of 8–12 compared to the initial undoped MnSi.

It is interesting to compare the experimentally determined critical index (points in Fig. 15b) with the standard values of β in the Ising, Heisenberg, and Landau models (lines *1–3* in Fig. 15b, respectively). The obtained data apparently exclude the Ising case, and for $0.05 \leqslant x \leqslant 0.4$ are rather grouped

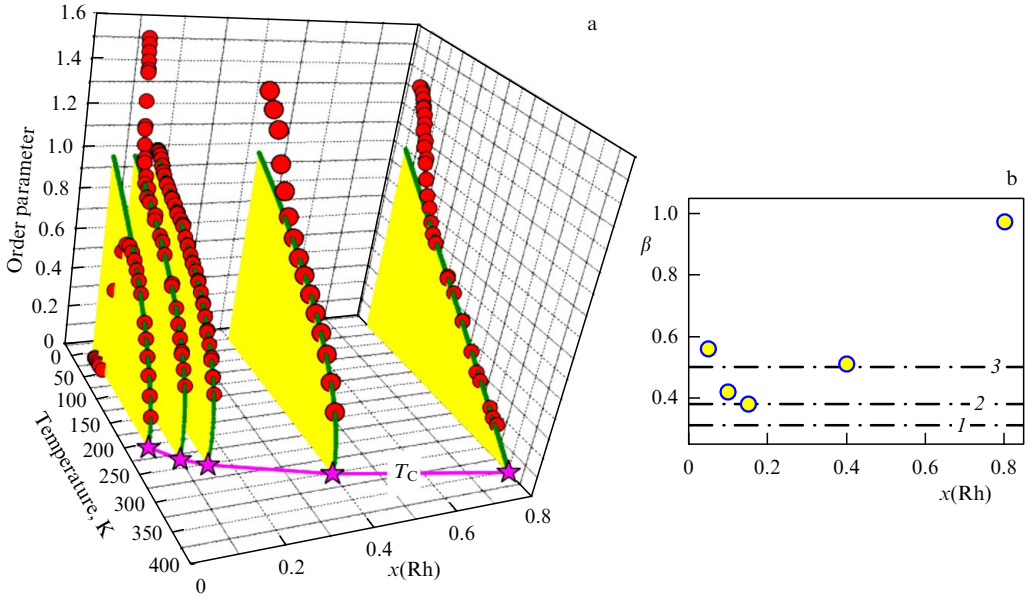

Figure 15. Temperature dependences of the order parameter in the $Mn_{1-x}Rh_xSi$ system (panel a) and the dependence of the critical index β on the rhodium concentration (panel b). The dashed-dotted lines correspond to theoretical models: *1* — Ising model, *2* — Heisenberg model, *3* — Landau mean field theory.

around the value of $\beta \sim 0.5$, typical of mean field theory. Moreover, for a sample with a rhodium concentration of $x = 0.8$, the critical index is $\beta = 0.97 \pm 0.02$ and differs from the standard values by a factor of 2–3 (Fig. 15b). Such unusual values of the critical index are likely associated with strong disorder and the formation of the Griffiths phase, but this issue requires further theoretical study and is beyond the scope of the present work.

Note that for $T < 100$ K, a new low-temperature growth region appears on the $M_0(T)$ curves, which is most pronounced for samples with $x = 0.1$, $x = 0.4$, and $x = 0.8$ (Fig. 15a). The possible nature of this low-temperature anomaly will be discussed further in Section 5.3.

4.4 Magnetic disorder and specific heat in $Mn_{1-x}Me_xSi$ (Me = Co, Fe, Rh)

The approach proposed in this paper for the description of the physical properties of $Mn_{1-x}Me_xSi$ (Me = Co, Fe, Rh) samples is based on the assumption of strong disorder, leading to clustering of the magnetic subsystem already in the composition range of $x \sim 0.05-0.1$. Moreover, in this concentration range, $Mn_{1-x}Fe_xSi$ retains a well-defined magnetic transition temperature, while the Curie point of $Mn_{1-x}Rh_xSi$ can be reliably determined even at higher alloying element concentrations of $x \sim 0.8$ (see Section 4.3 above). At first glance, this situation appears somewhat contradictory; however, it is important to keep in mind that different physical quantities may 'react' differently to disorder in the system.

A classic illustration of this thesis is the behavior of the specific heat in the presence of magnetic disorder. Figure 16 shows examples of the temperature dependences of the specific heat $C_p(T)$ for $Mn_{1-x}Me_xSi$ (Me = Co) from [49]. It is clearly seen that the sharp features of $C_p(T)$ for pure MnSi quickly blur upon the introduction of alloying elements replacing manganese. In this case, a broad maximum of $C_p(T)$ is observed in the vicinity of T_C, therefore, from the experimental data one can only estimate a certain characteristic temperature T_f associated with the spin-fluctuation transition (see Section 4.1), and determining T_C from the $C_p(T)$ curves requires a certain scientific courage. Note that the application of an external magnetic field in the range $H < 9$ T naturally leads to an additional blurring of the heat capacity maximum (Fig. 16).

From a theoretical perspective, the case of the influence of various impurities on the heat capacity, including nonmagnetic ones that dilute the magnetic subsystem, has been studied most thoroughly. In this case, the significant effects can arise even at a small concentration of impurities [38]. Let us cite a quote. "The reason why the influence of impurities on the critical behavior is expected to be significant is as follows. Suppose that we introduce several impurities into a system near the critical point, thereby including a small perturbation. The response to such a perturbation is described in terms of the behavior of various susceptibilities and correlation functions. Near the critical point of an ideal system, some of these quantities are large and represent singular functions of temperature. This means that a small amount of impurity can lead to large effects near the critical point, thereby significantly changing the critical behavior of a pure system. Critical exponents can also change. Smoothing out the singular behavior of some quantities is possible" ([38], pp. 198–199 of Russian edition; hereafter the quotes from [38] are given in the backward translation from the Russian edition). In particular, the use of the renormalization group technique in relation to the Ginzburg–Landau functional with random fields gives the general result that 'the presence of an impurity eliminates the divergence of the heat capacity' ([38], p. 208 of Russian edition).

However, the possibilities of an analytical description of this problem are apparently limited to the case of not too strong disorder [38]. To understand what the critical behavior of a system with strong disorder might look like, one can turn to the well-known results of studies of ferromagnetic metallic glasses [77–79]. These materials have a well-defined Curie point, which can be reliably determined from a study of the

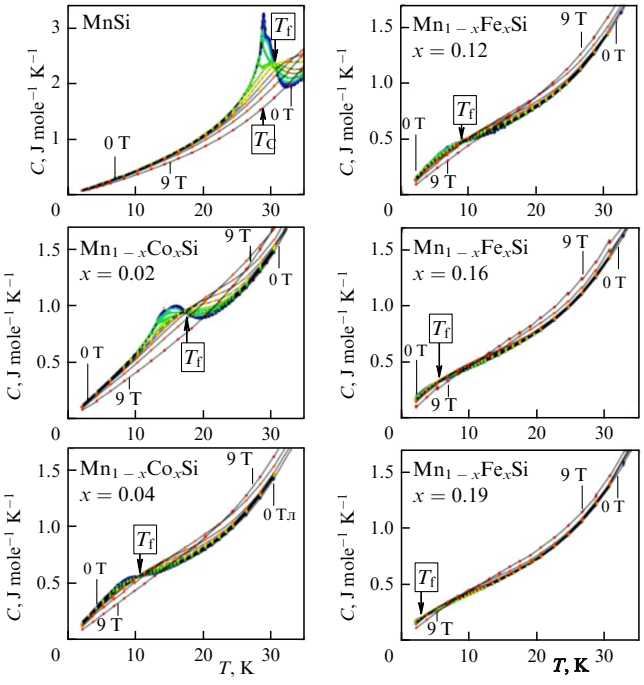

Figure 16. Temperature dependences of low-temperature specific heat in a magnetic field of up to 9 T in the $Mn_{1-x}Co_xSi$ and $Mn_{1-x}Fe_xSi$ systems. Arrows indicate the Curie temperatures T_C and the spin-fluctuation transition temperature T_f. (From [49].)

magnetic properties, and a strongly diffuse peak of the heat capacity, located in the temperature range slightly below the Curie temperature. Obviously, these experimental data, as well as the theoretical estimates given above, are in good qualitative agreement with the temperature dependences $C_p(T)$ for $Mn_{1-x}Me_xSi$ (Me = Co, Fe) (see Fig. 16).

Let us now consider the data we obtained on the specific heat for $Mn_{1-x}Rh_xSi$ (Fig. 17). Panel a illustrates the general course of the $C_p(T)$ curves for compositions with $x = 0.1$, $x = 0.15$, and $x = 0.8$. For comparison, the result of the specific heat measurement on MnSi single crystal is shown (curve for $x = 0$). It is evident that doping with rhodium suppresses the low-temperature peak of the specific heat, which is completely consistent with the data of magnetic measurements, according to which for $x > 0.1$ the transition to the spiral phase does not occur. It is interesting that in the MnSi sample we studied, the $C_p(T)$ feature associated with the magnetic transition is shifted downwards relative to the magnetic transition temperature, just as in metallic glasses (Fig. 17a); and the sharp feature of the heat capacity at $T = T_C$, observed for an MnSi single crystal in [49] (see Fig. 16), is absent in this case. Within the framework of existing theoretical concepts [38], it is natural to associate such a discrepancy with the different concentration of the defects of MnSi single crystals studied in various experiments.

The high-temperature ($T > 150$ K) regions of the temperature dependences of the heat capacity for samples with $x = 0.1$ and $x = 0.15$ exhibit broad, small-amplitude features arising in the region $T < T_C$, which may be associated with a ferromagnetic transition in a system with strong magnetic disorder (Fig. 17b). In this case, the broadening of the heat capacity peak for the sample with $x = 0.8$ turns out to be so strong that this feature does not exceed the measurement error of $C_p(T)$. This result is in complete agreement with both the experimental data for disordered ferromagnetic systems [77–79] and the theoretically expected effect of disorder on the specific heat singularity [38]. Note that the application of an external magnetic field $H = 9$ T does not affect the general course of the curves at $T > 150$ K and only leads to an additional broadening of the features associated with the ferromagnetic transition, as would be expected for second-order phase transitions.

Since the low-temperature magnetic transition, which could give an additional nonlinear contribution to the $C_p(T)$ dependence, does not occur in $Mn_{1-x}Rh_xSi$ with $x > 0.1$, a classical analysis of the low-temperature specific heat can be performed in coordinates $C_p/T = f(T^2)$ (Fig. 17c). In the simplest case, the reduced specific heat $C_p(T)$ should depend linearly on the square of the temperature T^2: $C_p/T = \gamma + bT^2$, where $\gamma = (\pi^2/3)\, g(E_F) k_B T$ and $b = (12\pi^4/5)(R/\Theta_D^3)$ are the coefficients included in the expressions for the electron $C_e = \gamma T$ and the low-temperature phonon $C_{ph} = bT^3$ specific heat, respectively. Here R is the universal gas constant, $g(E_F)$ is the density of states at the Fermi level, and Θ_D stands for the Debye temperature [80].

However, the experimental situation for $Mn_{1-x}Rh_xSi$ is more complex. Comparison of the $C_p(T)$ curves in zero magnetic field (Fig. 17c, curve *1*) and in a magnetic field $H = 9$ T (Fig. 17c, curve *2*) reveals the presence of a low-

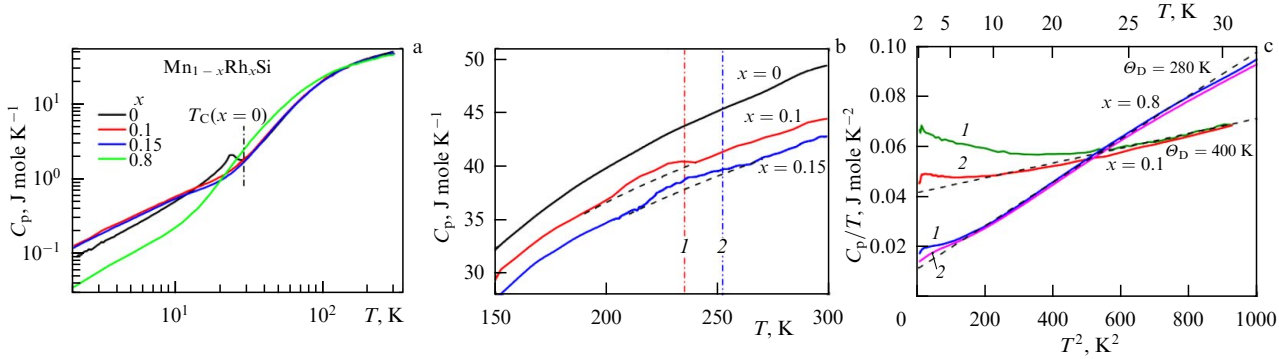

Figure 17. Temperature dependences of the specific heat for $Mn_{1-x}Rh_xSi$ samples with $x = 0$, $x = 0.1$, $x = 0.15$ and $x = 0.8$. (a) $C_p(T)$ dependences in a wide temperature range for zero magnetic field; (b) features of the heat capacity in the vicinity of the Curie temperature, the dash-dotted lines denote the Curie temperatures for samples with $x = 0.1$ (line *1*) and with $x = 0.15$ (line *2*). In the panel b, the $C_p(T)$ curves are shifted by 2 J mole K^{-1} for clarity. (c) Low-temperature heat capacity for the samples with $x = 0.1$ and $x = 0.8$ in zero magnetic field (curves *1*) and in a magnetic field of 9 T (curves *2*) in coordinates $C_p/T = f(T^2)$. The dashed lines correspond to the linear sections used to estimate the Debye temperature and the electron specific heat coefficient γ.

temperature magnetic contribution, the amplitude of which is suppressed by the magnetic field. This feature for the sample with $x = 0.1$ is observed at $T < 25$ K, while for the sample with $x = 0.8$, the magnetic contribution decreases in amplitude and this feature shifts down the temperature scale to the region $T < 10$ K. The decrease in the additional contribution to the specific heat in a magnetic field indicates its spin-fluctuation nature, since the external magnetic field orders the spin subsystem and, consequently, suppresses magnetic fluctuations. It should be noted that, in addition to this feature, in the region of $T \sim 2-5$ K, the $C_p(T)$ curves of $Mn_{1-x}Rh_xSi$ exhibit a small maximum, characteristic of a Schottky anomaly (Fig. 17c). This feature is weakly dependent on the magnetic field and is likely due to defects and/or impurities in the sample.

Linear approximation of the experimental data $C_p/T = f(T^2)$ for the temperature range where the magnetic contribution has little effect on the temperature dependence of the specific heat (dashed lines in Fig. 17c) made it possible to estimate the Debye temperature and the γ coefficient: $\Theta_D(x = 0.1) \sim 400$ K, $\gamma(x = 0.1) = 0.0416$ J mole K^{-2} and $\Theta_D(x = 0.8) \sim 280$K, $\gamma(x = 0.8) = 0.0113$ J mole K^{-2}. Thus, substitution of manganese by rhodium leads to a decrease in the Debye temperature in the $Mn_{1-x}Rh_xSi$ system. A change in the γ coefficient with a variation in the sample composition indicates a possible change in the electron concentration and density of states. It is easy to see that with an 8-fold change in the rhodium content from $x = 0.1$ to $x = 0.8$, the manganese concentration decreases from 0.9 to 0.2, i.e., by a factor of 4.5. The coefficient γ also decreases: $\gamma(x = 0.1)/\gamma(x = 0.8) \sim 3.7$. This result indicates that the observed change in the density of electron states is primarily due to a change in the relative concentration of manganese atoms in the $Mn_{1-x}Rh_xSi$ substitutional solid solutions.

5. The model of the magnetic properties of $Mn_{1-x}Rh_xSi$

In this section, we will demonstrate that the spin-polaron model mentioned above can be successfully applied to describe the magnetic properties of $Mn_{1-x}Rh_xSi$. To this end, we will briefly discuss the experimental motivation and basic physical assumptions underlying this approach, and present the main consequences of the theory. In this section, we will rely primarily on the results of [21].

5.1. The spin-polaron model

The spin-polaron model [21] was developed to describe two main features of the magnetic properties of transition metal silicides with ferromagnetic interaction. The most well-known anomaly characteristic of this class of materials is a significant discrepancy between the effective magnetic moment $\sim \mu_B$, determined from the Curie constant in the paramagnetic phase, and the saturation moment in the ferromagnetic phase, which turns out to be much smaller than the Bohr magneton per magnetic ion. This discrepancy is usually interpreted within the framework of the theory of itinerant magnetism [56], according to which this discrepancy is a consequence of the distributed (rather than localized on magnetic ions) spin density in the unit cell and the presence of strong spin fluctuations.

Another, less well-known feature of the magnetic properties of silicides is the nontrivial field dependence of the magnetization $M(B, T = \text{const})$ in the paramagnetic state. Approximation of the experimental data using the formula $M(B, T) = M_0\varphi(\mu^* B/k_B\theta(T))$, where $\theta(T)$ denotes a certain effective temperature, and the function $\varphi(x)$ describes the saturation of the field dependence and satisfies the relations $\varphi(x \to 0) = \alpha x$, $\varphi(x \to \infty) = 1$ and $d\varphi/dx > 0$, yields a small saturation magnetic moment M_0 per magnetic ion: $M_0 \ll \mu_B$. In this case, the effective magnetic moment μ^*, which determines the slope of $\partial M/\partial B$ in a weak magnetic field, turns out to be significantly greater than the Bohr magneton: $\mu^* \gg \mu_B$. For example, in the case of manganese monosilicide, MnSi, in the paramagnetic phase, the value of μ^* is $\sim (5-6)\mu_B$, and the saturation moment is of the order of $M_0 \sim 0.3\mu_B$/Mn [21, 58]. In the case of substitutional solid solutions $Fe_xCo_{1-x}Si$, the effective magnetic moment can reach $\mu^* \sim 13\mu_B$, while the parameter M_0 lies in the range of $(0.05-0.2)\mu_B$/Co [81, 82]. We emphasize that these experimental facts have no explanation in the theory of itinerant magnetism, which at finite temperatures is limited to considering the linear magnetic response, i.e., the magnetic susceptibility in the limit $H \to 0$.

The spin-polaron model was initially proposed to explain experimental data on magnetic resonance in MnSi [57–59]. The study of the dynamic magnetic properties clearly shows that the magnetic subsystem of manganese monosilicide consists of localized magnetic moments. This result is consistent with the results of LDA calculations, according to which the spin density of MnSi is localized on manganese ions and the value of such LMM is $\mu_{Mn} \approx 1.2\mu_B$ [60]. Thus, to explain the small value of the saturation magnetic moment, it is necessary to propose some mechanism for screening the manganese LMM. According to [57, 58], this effect is due to the formation of spin polarons around the Mn ions, which are quasi-bound states of itinerant electrons in the vicinity of the Mn ion, in which the spins of manganese and the spins of electrons are oriented antiparallel. Such a structure can be considered as a nanoscale ferrimagnet, and it can be shown that the dynamic magnetic properties expected in this model are in good agreement with experiment [57]. Within the spin-polaron approach, spin fluctuations (which determine, in particular, the width of the magnetic resonance line [57–59]) are caused by electron transitions between itinerant and quasi-bound states. This hypothetical construction is qualitatively depicted in Fig. 18a.

For a quantitative analysis of the magnetic properties of a spin polaron in an external magnetic field $\mathbf{H}$, it is necessary to introduce two magnetization vectors $\mathbf{M}_1$ and $\mathbf{M}_2$ one of which corresponds to the LMMs and the other to quasi-localized electrons. It is assumed that all three vectors lie in the same $x-y$ plane and the vector $\mathbf{H}$ is parallel to the y-axis (Fig. 18b). Regarding the magnetic interactions inside the spin polaron, which determine the orientation of $\mathbf{M}_1$ and $\mathbf{M}_2$, the following assumptions are made in [21]. (*1*) For any external magnetic field, the vectors $\mathbf{M}_1$ and $\mathbf{M}_2$ are parallel and codirected to the corresponding local fields $\mathbf{H}_1$ and $\mathbf{H}_2$. (*2*) The local fields $\mathbf{H}_1$ and $\mathbf{H}_2$ depend linearly on $\mathbf{M}_1$ and $\mathbf{M}_2$. (*3*) The total vector $\mathbf{M}_1 + \mathbf{M}_2$ is aligned along the external magnetic field $\mathbf{H}$ and, consequently, the projections satisfy the conditions (*4*) $M_{1x} + M_{2x} = 0$ and $M_{1y} + M_{2y} \neq 0$.

As in the standard semiclassical theory of ferrimagnetism [22], in [21] it is assumed that for the absolute values of magnetization the relation $M_{1,2} = M_{10,20}\varphi(\mu_{1,2}H_{1,2}/k_BT)$ is valid, where $\varphi(x)$ is some function common to the two magnetization vectors, describing the average spin polarization and $H_{1,2}$ are the amplitudes of the local fields acting on

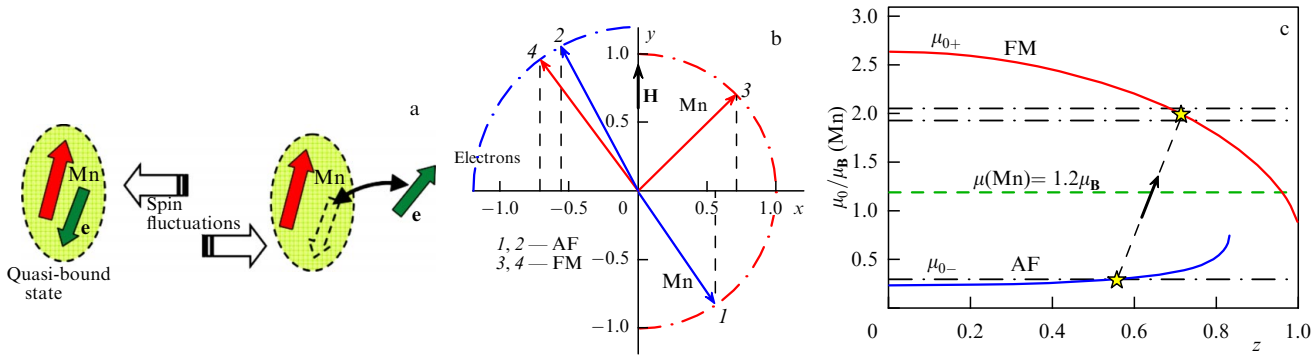

Figure 18. (a) Spin polaron and magnetic fluctuations; (b) configurations of magnetization vectors for the manganese LMM (*1*, *3*) and magnetic moments of quasi-bound electrons (*2*, *4*) for the AF geometry (blue arrows *1* and *2*) and for the FM geometry (red arrows *3*, *4*); (c) dependence of the saturation magnetic moment of the spin polaron on the parameter z in the AF geometry μ_{0-} and in the FM geometry μ_{0+}. The asterisks in panel c show the values of the saturation magnetic moments corresponding to the NMR data for $Mn_{1-x}Rh_xSi$ (dash-dotted lines); the expected transition from the AF state to the FM state is indicated by the arrow. The dotted line shows the LMM value of a single manganese ion according to the literature data [60]. In panel b, magnetization configurations *1*, *2* and *3*, *4* are shown for the μ_{0-} and μ_{0+} values, respectively, which are used to describe the NMR spectra. (Details are in the text.)

$\mathbf{M}_1$ and $\mathbf{M}_2$. Magnetizations $\mathbf{M}_1$ and $\mathbf{M}_2$ represent magnetic contributions from elementary magnetic dipoles μ_1 and μ_2, the total number of which in the spin polaron is n_1 and n_2, respectively, and, thus, the saturation magnetizations are $M_{10} = \mu_1 n_1$ and $M_{10} = \mu_2 n_2$.

Under the assumptions made, local fields are written as

$$\mathbf{H}_1 = \mathbf{H} + w_{11}\mathbf{M}_1 + w_{12}\mathbf{M}_2\,, \tag{17a}$$

$$\mathbf{H}_2 = \mathbf{H} + w_{21}\mathbf{M}_1 + w_{22}\mathbf{M}_2\,. \tag{17b}$$

Equations (17) are similar to standard expressions in mean field theory [22], but in our case w_{ij} are parameters describing magnetic interactions within the spin polaron that provide a given spin configuration. Let us consider the nontrivial case when $M_{1,2x} \neq 0$. Then, taking into account that $M_{1x} + M_{2x} = 0$, we can write the conditions for the parallel alignment of the magnetization vectors to the local fields

$$w_{12}(M_{1y} + M_{2y}) + H = 0; \quad w_{12} = w_{21}\,, \tag{18}$$

which, according to the assumptions made, must be fulfilled for any values of the external magnetic field H. In a weak magnetic field, the total magnetization of the spin cluster will be $M = M_{1y} + M_{2y} = \chi H$ and, therefore, the parameters w_{12} and w_{21} turn out to be a function of the temperature $w_{12} = w_{21} = -1/\chi(T)$. However, if the magnetization is close to saturation, Eqn (4) gives the field dependence of the parameters $w_{12} = w_{21} = -H/M_0$, where M_0 is the total saturation magnetic moment of the spin polaron. Thus, the requirement for the parallel alignment of $\mathbf{M}_1 || \mathbf{H}_1$ and $\mathbf{M}_2 || \mathbf{H}_2$ for an arbitrary H in the approximation under consideration is equivalent to the condition $w_{12} = w_{21} = -H/M(H, T)$, and the model parameters w_{12} and w_{21} turn out to be functions of the temperature and magnetic field. Note that in the standard mean field theory, the parameters w_{ij} are reduced to numerical coefficients in formulas like (17) [22].

Relation (18) and the condition $M_{1x} + M_{2x} = 0$ give the following expression for the amplitudes of local fields

$$H_1 = M_1\left(w_{11} + \frac{H}{M}\right) \tag{19a}$$

and

$$H_2 = M_2\left(w_{22} + \frac{H}{M}\right). \tag{19b}$$

Then the magnetizations M_1 and M_2 take the form:

$$M_1 = M_{10}\varphi\left(\mu_1 M_1 \frac{[w_{11} + H/M]}{k_B T}\right), \tag{20a}$$

$$M_2 = M_{20}\varphi\left(\mu_2 M_2 \frac{[w_{22} + H/M]}{k_B T}\right). \tag{20b}$$

In [21], the canted ferrimagnetic type orientation of the vectors $\mathbf{M}_1$ and $\mathbf{M}_2$ was considered, when the projections M_{1y} and M_{2y} have opposite signs (hereinafter referred to as 'AF geometry,' Fig. 18b, blue arrows *1* and *2*). It is also easy to consider the case when the projections M_{1y} and M_{2y} are of the same sign (Fig. 18b, red arrows *3* and *4*). For such an arrangement of the magnetization vectors $\mathbf{M}_1$ and $\mathbf{M}_2$, the designation 'FM geometry' will be used.

The next important step in constructing the spin polaron model is the requirement of identical equality of the arguments of the function φ: $M_{1,2} = M_{10,20}\varphi(y)$, where $y = \mu_1 M_1[w_{11} + H/M]/k_B T \equiv \mu_2 M_2[w_{22} + H/M]/k_B T$ [21]. In this case, the relations

$$w_{11} = w_{22} = w\,, \tag{21}$$

$$\mu_1 M_1 = \mu_2 M_2\,, \tag{22}$$

must be satisfied and, in addition, the proportion $M_1/M_2 = M_{10}/M_{20}$ will be valid for any temperature values. The equality of the arguments generally ensures the smoothness of the field dependence of the derivative $\partial M/\partial H = f(H)$ for the magnetic response of the spin polaron as a whole. For AF geometry, the validity of the condition $\partial M/\partial H > 0$ within the framework of the problem under consideration, can be interpreted as the condition for the thermodynamic stability of the spin polaron [21]. According to [83], when considering the stability of a paramagnet, in addition to the obvious condition for the isothermal susceptibility $\chi(H \to 0) \geqslant 1/4\pi$, it is necessary to

take into account the condition on the caloric equation of state, which, at not too low temperatures and finite magnetic field values, imposes a restriction on the sign of the derivative $\partial M/\partial H > 0$ [21]. As long as we consider the AF geometry and FM geometry of the spin polaron from a single point of view, we will assume that conditions (21) and (22) are satisfied in both cases.

We require that for any possible spin configuration of the vectors $\mathbf{M}_1$ and $\mathbf{M}_2$ the condition $M_{2y} > 0$ be fulfilled and introduce the notation: $z = M_{2x}/M_2$ and $s = M_{10}/M_{20}$. Then the magnetization of the spin polaron is given by the expression:

$$M(H,T) = M_{20} f_{\pm} \varphi\left(\frac{\mu_2 M_2}{k_B T} w + \frac{\mu_2 H}{f_{\pm} k_B T}\right), \tag{23}$$

where the functions f_+ and f_- have the following form:

$$f_{\pm}(z,s) = \sqrt{1-z^2} \pm \sqrt{s^2 - z^2}\,. \tag{24}$$

In Equation (24), the '+' and '-' signs correspond to the FM and AF types of magnetization vector alignment in the spin polaron, respectively. Note that, due to the condition (22), the parameter s can also be represented as $s = \mu_2/\mu_1$ and $s = \sqrt{n_1/n_2}$. It is easy to verify that, in the region of the linear magnetic response $\varphi(y) \approx \alpha y$, the magnetization of the spin polaron does not depend on the function f_+ or f_-

$$M \approx \chi H = \alpha \frac{M_{20}\mu_2}{k_B(T - T^*)} H, \tag{25a}$$

$$T^* = \frac{M_{20}\mu_2 w}{k_B}. \tag{25b}$$

Therefore, in a weak magnetic field, a spin polaron possesses a Curie–Weiss magnetic susceptibility χ of the ferromagnetic type. For the above-considered approximations of $\varphi(y)$ by the Brillouin function for spin S = 1/2 and Langevin function, the numerical coefficient α is equal to 1 and 1/3, respectively. It can be noted that in Eqn (23), the second term in the argument of the function φ will dominate when the inequality $w \ll H/M_2 f_{\pm}$ is satisfied, which, for the linear response region, is equivalent to the condition on the temperature $T \gg 2T^*$. As a result, there always exists a region of parameters for a spin polaron, where a good approximation for the magnetization is an interpolation formula of the form $M \approx M_0^* \varphi[\mu^* H/k_B(T - T^*)]$ with renormalized saturation magnetization and effective magnetic moment: $M_0^* = M_{20} f_{\pm}$ and $\mu^* = \mu_2/f_{\pm}$.

If the LMMs of electrons and magnetic ions are close in amplitude $\mu_1 \sim \mu_2$, then the condition $f_- \ll 1$ (Eqn (24)) will be satisfied for the AF geometry, resulting in $M_0^* \ll n_{1,2}\mu_{1,2}$ and $\mu^* \gg \mu_{1,2}$. At the same time, the magnetic susceptibility will imply a magnetic moment of $\sim \mu_{1,2}$ (Eqn (25a)). This relationship between the parameters is characteristic of so-called weak itinerant magnets; however, the spin-polaron model has an advantage because it explains not only the decrease in saturation magnetization but also the large value of μ^*, as well as the reason why the LMM value characteristic of a magnetic ion is found experimentally from the Curie constant. Furthermore, in our case, the Curie–Weiss law proves to be exact. Note that in Moriya's theory [56] the problem of anomalous values of μ^* appearing in the argument of the function φ is not solved in any way, the Curie constant is not related to the value of any LMM or saturation magnetization, and the Curie–Weiss law is satisfied only approximately. Thus, the paradoxical properties of 'weak itinerant magnets' may well find an alternative (and possibly more consistent) explanation in the spin-polaron model, in which both the interaction effects of itinerant electrons and localized magnetic moments, as well as spin fluctuations, are significant. The special role of spin fluctuations can be seen if we rewrite the condition (22) of equality of the arguments of the function φ in the form $n_1/n_2 = (\mu_2/\mu_1)^2$. At first glance, the ratio of the number of LMMs and electrons in a spin polaron n_1/n_2 should be a ratio of integers, while the quantity $(\mu_2/\mu_1)^2$ in a real experimental system, in general, will not be a rational number. However, according to [21], when taking spin fluctuations into account, the ratio n_1/n_2 will include an *integer* number of LMMs in the spin polaron and the *average* number of electrons, depending on the probability of transitions between quasi-bound and itinerant states.

Previously, the spin-polaron model for the AF geometry case was successfully applied to the quantitative description of the temperature and field dependences of magnetization in MnSi [21], as well as to the explanation of the characteristics of localized magnetic moments on the surface of the topological Kondo insulator SmB_6 [59]. Below, we consider a possible explanation for the magnetic properties of $Mn_{1-x}Rh_xSi$ within the framework of this approach, including the effect of a giant increase in the Curie temperature.

5.2 The features of the magnetic properties of $Mn_{1-x}Rh_xSi$ in the spin-polaron model

Following the work [21], we begin with a description of the magnetic properties of MnSi. Since $\mu_{Mn} > \mu_e$ [60], then for the paramagnetic response in the AF geometry (the function f_- is positive), it is necessary to assume that the magnetization $\mathbf{M}_1$ is created by n_1 LMMs of manganese, and the magnetization $\mathbf{M}_2$ corresponds to the contribution of n_2 electrons. In this case, the saturation magnetic moment of the spin polaron per manganese ion μ_{0-} and the effective magnetic moment μ^* will be equal to

$$\mu_{0-} = \frac{\mu_{Mn}^2}{\mu_e} f_-\left(z, \frac{\mu_e}{\mu_{Mn}}\right), \tag{26a}$$

$$\mu^* = \frac{\mu_e}{f_-(z, \mu_e/\mu_{Mn})}. \tag{26b}$$

When deriving Eqn (26), we took into account condition (22). From the experimental field dependences of magnetization at different temperatures, it is possible to find the parameters μ_{0-} and μ^*, which in the paramagnetic phase of MnSi are $\mu_{0-} = (0.3 \pm 0.01)\mu_B$/Mn and $\mu^* = (5.3 \pm 0.2)\mu_B$ [21]. Note that in the spin polaron model, the product of μ_{0-} and μ^* does not depend on the magnetic moment of the electron and the function f_-: $\mu_{0-}\mu^* = \mu_{Mn}^2$ (Eqn (26)), and the presented experimental data give the estimate $\mu_{Mn} = (1.2-1.3)\mu_B$, which is in good agreement with the results of LDA calculations, according to which $\mu_{Mn} = 1.2\mu_B$ [60]. If we accept that $\mu_e = \mu_B$, then Eqn (26a) and (26b) give practically coinciding estimates: $f_- = 0.17-0.21$ and $f_- = 0.18-0.21$. Thus, the $M(H,T)$ experimental data confirm the applicability of the spin-polaron model for describing the magnetic properties of MnSi [21]. As long as the values of f_- and $s = \mu_{Mn}/\mu_e$ are known, Eqn (24) allows one to find the parameter z and determining the configuration of the vectors

$\mathbf{M}_1$ and $\mathbf{M}_2$ in the spin polaron. For example, from Fig. 18c it is evident that the equality of μ_{0-} to the experimental value $0.3\mu_B$/Mn will be achieved at $z = 0.56$. The spin configuration corresponding to this case is shown in Fig. 18b (blue arrows *1* and *2*).

The obtained data give an estimate of the ratio of the average number of electrons to the number of manganese LMMs in the spin polaron of MnSi: $n_e/n_{Mn} = (\mu_{Mn}/\mu_e)^2 = 1.44-1.69$. In [21], it was proposed that the spin polaron is formed by three electrons and two manganese ions, for which $n_e/n_{Mn} = 1.5$, in agreement with experiment. Possible deviations from this ideal ratio, as noted above, may be due to spin fluctuations caused by electron transitions from spin-polaron to itinerant states. Interestingly, a study using inelastic neutron scattering led the authors of a recent paper [84] to the conclusion that, in describing the magnetic properties of MnSi, it is necessary to consider bound triplets of manganese LMMs rather than individual magnetic ions. This result not only agrees qualitatively with the spin-polaron model but can also be quantitatively compared with experimental data for $n_{Mn} = 3$ and $n_e = 5$ ($n_e/n_{Mn} \approx 1.67$).

The above estimates of n_e and n_{Mn} indicate that the size of the spin polaron in MnSi must be smaller than or of the order of the lattice constant a. Thus, our model considers small-radius spin polarons, in contrast to giant magnetic polarons and ferrons [85, 86], in which the number of spins can reach hundreds of thousands [86]. In such a situation, the small-radius spin polaron in MnSi can be considered as a renormalized magnetic moment localized on the scale $\leqslant a$. Despite the fact that the spin polaron model is primarily justified by experimental data for the paramagnetic phase, such an interpretation of localized magnetic moments in MnSi turns out to be very fruitful for describing electron paramagnetic resonance and static magnetic properties in magnetically ordered phases [54, 57–59, 71]. For example, the period of the magnetic spiral in MnSi significantly exceeds the lattice constant and, therefore, the spiral phase can be formed by spin polarons. Manganese monosilicide is characterized by a sharp phase boundary between the paramagnetic and field-induced ferromagnetic (spin-polarized) phases [58], which cannot exist in the case of a conventional ferromagnet [22]. This contradiction is also explained by the spin-polaron model [58]. The spin-fluctuation transition in the spiral conical phase at ~ 15 K discovered in MnSi [87] is so far from the magnetic transition temperature of ~ 29 K that its occurrence requires an additional 'degree of freedom,' which is absent for 'conventional' LMMs of manganese, but naturally occurs in the two-component magnetic system of a spin polaron [87]. Next, we will show that it is the spin-polaron model that allows us to explain the nontrivial magnetic properties of not only MnSi, but also of $Mn_{1-x}Rh_xSi$, including data on nuclear magnetic resonance.

As shown in Section 4.2, the substitution of manganese by rhodium significantly affects the NMR spectra in zero external magnetic field (see Section 4.2 and Fig. 11). At low temperatures, when the spin polaron magnetization is close to saturation, formula (26a) can be used to estimate the magnetic moment in the AF geometry per manganese ion and, consequently, $\mu_1 \approx \mu_{0-} = 0.3\mu_B$/Mn in accordance with experiment. This estimate is valid for both pure MnSi and $Mn_{1-x}Rh_xSi$ samples in the region of low rhodium concentrations. At $x = 0.025$, this NMR signal coexists with the resonance response from the magnetic moments $\mu_2 \sim 1.2\mu_B$/Mn and $\mu_3 \sim 2\mu_B$/Mn. A further increase in the rhodium content leads to suppression of the signal with $\mu_1 \sim 0.3\mu_B$/Mn, and only features caused by $\mu_2 \sim 1.2\mu_B$/Mn and $\mu_3 \sim 2\mu_B$/Mn remain in the spectrum (see Fig. 11).

It is noteworthy that the magnetic moment $\mu_2 \sim 1.2\mu_B$/Mn, according to calculations [60], should be interpreted as a localized moment of an unshielded single manganese atom. Therefore, if, despite all the above-mentioned contradictions of the itinerant model, we consider that pure MnSi is an itinerant magnet with $\mu_1 \sim 0.3\mu_B$/Mn, then it must be recognized that for $Mn_{1-x}Rh_xSi$ at $x = 0.025$, the itinerant magnetism begins to transform into the magnetism of Heisenberg LMMs, and this transformation ends already at $x = 0.05$ (see Fig. 11). This possibility cannot be completely ruled out, but it would require the 'weak itinerant magnet MnSi' to be weak enough for a small concentration of rhodium impurity atoms to cause a radical redistribution of the spin density in the unit cell and the disappearance of spin fluctuations. In our opinion, this MnSi doping scenario is extremely unlikely.

From the spin-polaron model perspective, the transition from $\mu_1 \sim 0.3\mu_B$/Mn to $\mu_2 \sim 1.2\mu_B$/Mn and $\mu_3 \sim 2\mu_B$/Mn means that the AF geometry becomes unstable upon rhodium doping. As a result, some of the quasi-localized electron states in the vicinity of the LMM of manganese are destroyed, and some spin polarons undergo the change AF → FM in the arrangement of magnetizations. In the first case, an NMR signal with $\mu_2 \sim 1.2\mu_B$/Mn arises, while the signal with $\mu_3 \sim 2\mu_B$/Mn can be associated with a spin polaron in the FM geometry:

$$\mu_3 \approx \mu_{0+} = \mu_{Mn} f_+\left(z, \frac{\mu_{Mn}}{\mu_e}\right). \tag{27}$$

For $\mu_3 \sim 2\mu_B$/Mn, Eqn (27) allows one to find the parameter z (Fig. 18c) and determine the alignment of the magnetizations in the spin polaron with FM geometry (red arrows *3* and *4* in Fig. 18b). From Fig. 18b it is evident that for the AF → FM transition, the position of the magnetization vector for electrons changes only slightly, while for the LMM of manganese a spin-flop transition occurs.

The performed analysis shows that the spin-polaron model does not require exotic assumptions such as a change in the charge and spin state of the manganese ion, the presence of additional magnetic phases, and the acquisition of a magnetic moment by the nonmagnetic rhodium ion, which were used for the explanation of the NMR data [15]. However, the proposed interpretation means that below the Curie temperature, the $Mn_{1-x}Rh_xSi$ system is effectively two-phase. We assume that the first phase is the above-introduced ferromagnetic clusters that form the Griffiths phase and consist of spin polarons with FM geometry and a renormalized local magnetic moment of $\sim 2\mu_B$. The other phase surrounding the clusters is a paramagnetic metal with manganese ions, the magnetic moment of which is $\sim 1.2\mu_B$. As already noted, this 'construction' of the Griffiths phase is confirmed by the EPR data. Since in $Mn_{1-x}Rh_xSi$ the magnetic subsystem of manganese ions is diluted by nonmagnetic rhodium ions, it can be expected that ferromagnetic clusters correspond to spatial regions with the maximum content of manganese ions, in which rhodium ions are impurities, and the paramagnetic metal is formed by regions with a higher rhodium content, in which magnetic manganese ions are diluted.

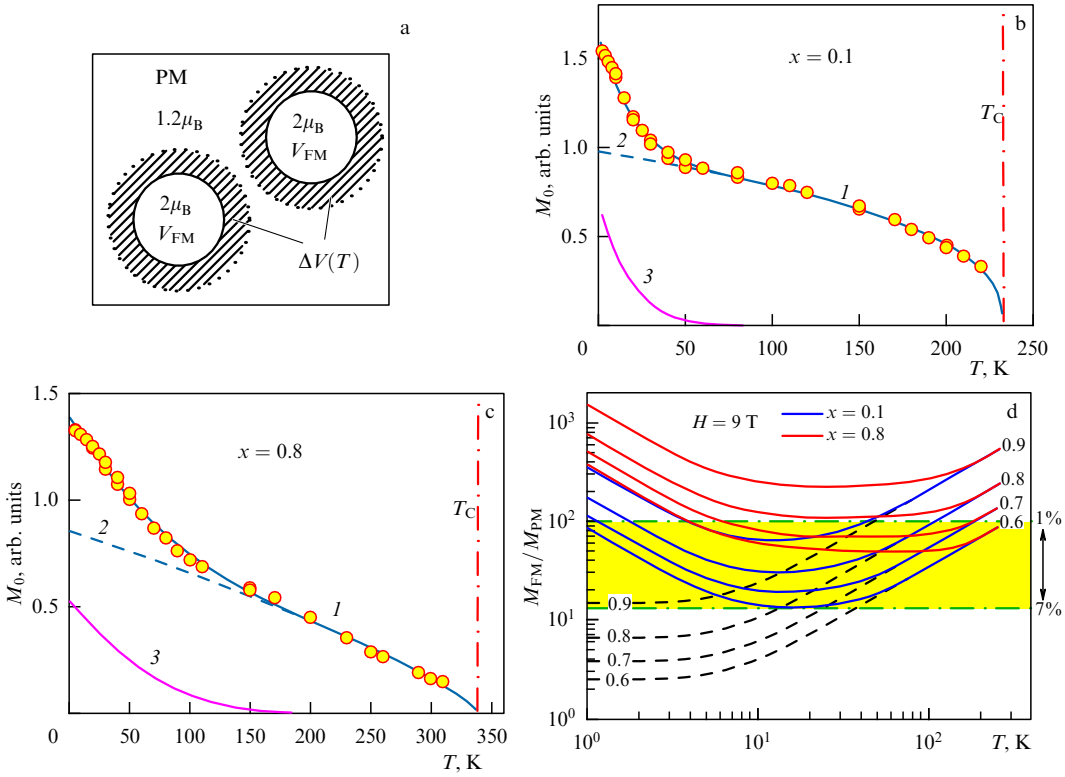

Figure 19. Model for describing the static magnetic properties of $Mn_{1-x}Rh_xSi$: (a) two-phase structure of the Griffiths ferromagnetic phase and an increase in the ferromagnetic cluster size with decreasing temperature; (b, c) temperature dependence of the order parameter for samples with $x = 0.1$ and $x = 0.8$; (d) estimated ratio of the contribution of the ferromagnetic cluster to the contribution of the paramagnetic phase in the magnetization of the sample in a magnetic field of 9 T; the numbers near the curves correspond to the fraction of the ferromagnetic phase in the sample volume (solid lines). In panels b, c, the dots denote the experimental data, *1* — calculation within the framework of the two-phase model, dashed line *2* — temperature dependence of the order parameter without taking into account the effect of increasing the cluster size, *3* — contribution due to a change in the cluster size caused by the suppression of spin fluctuations. In panel d, the dotted line shows the temperature dependence of the M_{FM}/M_{PM} ratio for the case where there is no increase in the cluster size and the initial content of ferromagnetic clusters is retained in the sample.

This qualitative description of the magnetic properties of $Mn_{1-x}Rh_xSi$ is well suited for NMR, but creates certain difficulties for interpreting the static magnetization. Indeed, we demonstrated above that at $T < T_C$, the power-law dependences of magnetization are well described by a single magnetic contribution from ferromagnetic clusters, whereas a sample with two magnetic phases should exhibit two contributions to the field and temperature dependences of magnetization.

Let us examine this issue in more detail. In [76], the ferromagnetism arising in a system of spin polarons in a ferromagnetic Kondo lattice model was considered using the Monte Carlo method. Numerical calculations show that in this case, at $T < T_C$, the size of the spin polaron increases with decreasing temperature, and at a certain temperature below the Curie temperature, individual magnetic polarons merge into a spatially homogeneous ferromagnetic phase via a percolation transition [76]. Interestingly, in this model, a broad maximum of the heat capacity arises in the region of temperatures below the Curie temperature, which corresponds to the experiment for the classical material with spin polarons EuB_6 [76].

In our Griffiths phase model, taking into account spin-polaron states, one can also expect an increase in the ferromagnetic cluster volume $V_{FM}(T) = V_0 + \Delta V_{FM}(T)$ due to the temperature-dependent addition $\Delta V_{FM}(T)$ (Fig. 19a). The possible nature of this phenomenon can be understood as follows. At high temperatures, spin fluctuations hinder the formation of spin polarons with FM geometry from the paramagnetic phase surrounding the ferromagnetic cluster. The ferromagnetic cluster 'tends' to polarize the adjacent region of the paramagnetic phase and, thus, increase its size. However, such ordering is hindered by spin fluctuations in the paramagnetic part of the sample. As the temperature decreases, the spin fluctuations 'freeze' and spin polarons with an effective moment $\mu_{0+} = 2\mu_B$ are formed around the magnetic manganese ions, which are attached to the ferromagnetic clusters. As a result, the size of the FM cluster and its saturation magnetization M_0 increase. This effect will result in a deviation of the temperature dependence of the order parameter from the simple critical behavior given by Eqn (13), as long as the relation $M_0 \sim (1 + \Delta V_{FM}(T)/V_0)(T_C - T)^\beta$ will hold as the cluster volume changes.

The low-temperature growth region on the $M_0(T)$ curves for $T < 100$ K, which is most pronounced for samples with $x = 0.1$, $x = 0.4$ and $x = 0.8$, may be associated with this effect (Fig. 15 and Fig. 19b, c). An alternative explanation was proposed in [16], where this feature was associated with the possible formation of a new low-temperature ferromagnetic phase. However, as follows from Fig. 14a, b, the isotherms of the field dependences of magnetization, reconstructed in rectifying coordinates $H/M = f(H^\xi)$, do not have qualitative differences in the regions $T > 100$ K and $T < 100$ K. Our EPR experiments also did not confirm the existence of a second ferromagnetic phase. Thus, the low-temperature feature of $M_0(T)$ apparently reflects a change in

the properties of the same cluster system in which a ferromagnetic transition with large values of $T_C > 200$ K is observed.

Let us consider the possibility of realizing in $Mn_{1-x}Rh_xSi$ the theoretical scenario proposed in [76], where the low-temperature features of magnetization are caused by percolation through the system of ferromagnetic clusters. In this case, the temperature of the onset of low-temperature growth $T_L \sim 100$ K will correspond to the percolation threshold, and the additional percolation contribution to the temperature dependence of the order parameter in the vicinity of the transition point will have the form $\Delta M \sim (T_L - T)^{\beta_L}$, where $\beta_L \sim 0.4$ is the critical index for the probability of belonging to an infinite cluster [88]. Processing of experimental data within the framework of this approach yields values of $\beta_L \sim 2$, therefore it is difficult to relate the observed low-temperature anomaly to the percolation threshold.

Now we consider the possible form of $\Delta V_{FM}(T)$ arising due to the suppression of spin fluctuations. If ΔV_0 is the maximum possible amplitude of the change in the additional contribution, then it is possible to $\Delta V(T) = \Delta V_0\, p_{FM}(T)$, where $p_{FM}(T)$ denotes the probability for a spin from the paramagnetic phase to attach to a ferromagnetic cluster. The form of the function $p_{FM}(T)$is unknown, but it can be expected that it should satisfy the conditions $p_{FM}(T_C) = 0$ and $p_{FM}(T = 0) = 1$. If the spin fluctuations are thermally activated, then the Arrhenius law $p_{FM}(T) = p_0 \exp(E_a/T)$ with the activation energy E_a can be chosen as the initial approximation. To satisfy the condition $p_{FM}(T_C) = 0$, the exponent may be modified: $p_{FM}(T) = p_0 \exp[E_a/(T - T_C)]$. Since $p_{FM}(0) = 1$, then $p_0 = \exp(E_a/T_C)$ and, as a result, we find $p_{FM}(T) = p_0 \exp[E_a T/T_C(T - T_C)]$.

Comparison with experimental data for $Mn_{1-x}Rh_xSi$ samples with $x = 0.1$ and $x = 0.8$ shows that the model function $M_0 \sim \{1 + (\Delta V_0/V_0) \exp[E_a T/T_C(T - T_C)]\} \times (T_C - T)^{\beta}$ provides a good description of the $M_0(T)$ data over the entire temperature range, including the low-temperature region (Fig. 19b, c). The activation energy depends on x and is equal to $E_a(x = 0.1) \sim 0.22$ eV and $E_a(x = 0.8) \sim 0.11$ eV, and the volume fraction of the ferromagnetic cluster phase is ~ 0.4. Note that the correction associated with $\Delta V_{FM}(T)$ in the vicinity of the Curie temperature is exponentially small and has virtually no effect on the previously found Curie temperature T_C and critical index β (Fig. 15).

Let us consider the maximum field $H = 9$ T, which limits the range of magnetization measurements in [16]. To estimate the contribution of the paramagnetic phase to the total magnetization, we neglect the effects of disorder and assume that $M_{PM} \sim \mu_{Mn} \tanh(\mu_{Mn} H/k_B T)$, and the ferromagnetic clusters formed by spin polarons are magnetized to saturation $M_{FM} \sim 2\mu_B$. The M_{FM}/M_{PM} ratio estimated in this way for different volume fractions of ferromagnetic clusters is shown in Fig. 19d by solid lines for samples with a rhodium content of $x = 0.1$ and $x = 0.8$. In carrying out the calculations, the $p_{FM}(T)$ functions obtained from processing the $M_0(T)$ data (Fig. 19b, c) were used. It is visible that only for the sample with $x = 0.1$ with a volume fraction of the cluster ferromagnetic phase of 0.4 the maximum contribution of the paramagnetic phase occurs in the range of 8–20 K and does not exceed 7%. In all other temperature ranges, the paramagnetic contribution for this sample is significantly smaller. For the sample with $x = 0.8$, the situation is even better, and the maximum error associated with the paramagnetic phase does not exceed 2%. Note that the found M_{FM}/M_{PM} ratio is a lower estimate, and in fields below 9 T, the paramagnetic contribution to the total magnetization is even smaller. Thus, even in a two-phase sample with a relatively high paramagnetic phase content, the contribution from the ferromagnetic cluster phase to the total magnetization will dominate, and, as a result, our analysis of the magnetic properties in the Griffiths phase cluster model is correct. Note that this statement is only valid for a scenario with increasing cluster size. If the cluster size does not increase and the volume fraction of ferromagnetic clusters remains unchanged, then the condition $M_{FM}/M_{PM} \gg 1$ will be satisfied only in the region $T > 30-50$ K, and at lower temperatures the contribution of the paramagnetic phase to the total magnetization will need to be taken into account (dashed lines in Fig. 19d).

5.3 The nature of the giant increase in the Curie temperature

The observed T_C increase in $Mn_{1-x}Rh_xSi$ is quite unusual and requires discussion of the possible mechanisms of magnetic interactions responsible for this phenomenon. Since rhodium doping leads to an increase in the lattice constant (see Fig. 10), the possible influence of 'negative chemical pressure' should be considered. Pressure itself, whether positive or negative, does not introduce additional magnetic disorder and exerts an effect through various microscopic parameters that determine the magnetic state. In the case of MnSi, external (positive) pressure suppresses the magnetic transition and induces the appearance of a quantum critical point unrelated to the Griffiths scenario [66]. Negative pressure is usually of the chemical nature and is realized by introducing various impurities that increase the lattice constant. In this case, both structural and magnetic disorder are simultaneously introduced into the system. With such a 'negative chemical pressure,' the possible growth factor T_C (the deformation field increasing the lattice constant) and the Griffiths mechanism of decreasing the magnetic transition temperature will act simultaneously.

Now we turn to the estimate of the possible effect of the influence of 'negative chemical pressure' for $Mn_{1-x}Rh_xSi$, neglecting the influence of disorder. For this purpose, we compare the literature data on the dependence of T_C on the lattice constant, obtained under conditions of high hydrostatic pressure [66] (region 1 in the inset in Fig. 20) with the data on the effect of aluminum, gallium, and germanium impurities on the Curie temperature [72]. In the latter case, both T_C and the lattice constant increase (region 2 in the inset in Fig. 20), and the data on hydrostatic pressure and 'negative chemical pressure' are in good agreement with each other. The results of [66, 72] can be extrapolated to the range of lattice constants for $Mn_{1-x}Rh_xSi$ samples and compared with the $T_C(x)$ data for this material. From Fig. 20 it follows that the ferromagnetic transition temperatures expected from the effect of 'negative chemical pressure' turn out to be 1.6–4.9 times lower than the experimental values. The maximum discrepancy is observed for the sample with $x = 0.05$, for which the change in the lattice constant is in the range studied for samples with 'negative chemical pressure' in [72]. Since the results from [72] for compositions with a low concentration of impurity atoms were used for the calculation of the expected effect, the extrapolated T_C values should be considered as an upper estimate, since magnetic disorder leading to the formation of the Griffiths phase generally reduces the Curie temperature. Thus, the effect of negative chemical pressure,

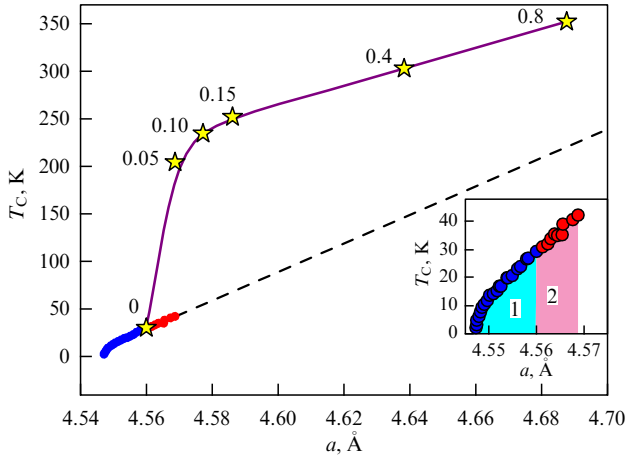

Figure 20. The effect of high hydrostatic pressure and 'negative chemical pressure' on the Curie temperature of MnSi and experimental data for the $Mn_{1-x}Rh_xSi$ system. Blue dots and area 1 in the inset are experimental data from [66] on the effect of the hydrostatic pressure, red dots and area 2 in the inset are the results for 'negative chemical pressure' from [72]. Asterisks are experimental $T_C(x)$ data for $Mn_{1-x}Rh_xSi$. The numbers near the asterisks correspond to the rhodium concentration x.

although 'working in the right direction,' cannot explain the observed T_C values; it predicts Curie temperatures 130–160 K lower than the experimental ones (see Fig. 20).

As already noted, the Moriya theory [56] has been widely used to explain the magnetic properties of MnSi. It assignes MnSi to the class of weak itinerant magnets with a spin density distributed over the entire unit cell [56]. In this case, the Curie temperature depends on the exchange integral and the saturation magnetization at zero temperature [89]: $T_C \sim JM_0(T=0)^2$. From Fig. 3 it is evident that for $Mn_{1-x}Rh_xSi$ the parameter $M_0(T=0)$ is the same as that of the original MnSi material, or slightly smaller. Therefore, if we remain within the framework of the itinerant magnetism theory, then to explain the observed increase in T_C from 29 K ($x=0$) to 352 K ($x=0.8$) it is necessary to require a change in the value of J (that is, in fact, the Coulomb energy of electrons in the system) by at least a factor of 12. This possibility seems extremely unlikely. Strictly speaking, the same problem arises in the case of magnetism of localized magnetic moments of the Heisenberg type, since in this case $T_C \sim J\mu_{Mn}^2$ [22, 66], and for $\mu_{Mn} = \text{const}$, a significant change in the exchange energy is required.

In this situation, it is appropriate to ask in what other systems a strong (and perhaps somewhat unexpected) increase in the Curie temperature has been observed. These effects are known to arise repeatedly in dilute magnetic semiconductors [13–14, 90–102]. In this class of compounds, most of the studies are carried on the silicon Si⟨Mn⟩ films with introduced magnetic manganese ions [90–96]. For such materials, the T_C value lies in the range of 200–800 K, depending on the manganese content, which varies from fractions of an atomic percent to ten atomic percent. An enhancement of the ferromagnetic properties is also characteristic of Ge⟨Mn⟩ films, for which the Curie temperature is ~ 300 K for a manganese concentration of ~ 5 at.% [97]. In GaAs⟨Mn⟩ films, T_C values of $\sim 100-200$ K have been observed [13, 14, 98]. Some dilute magnetic semiconductors were produced by high pressure-high temperature treatment [99-102]. In the case of the samples synthesized by this technique, the ferromagnetic transition for GaSb⟨Mn⟩ occurs at $T_C \sim 280$ K [99–101], and for GaSb⟨Cr⟩ the Curie temperature $T_C \sim 350$ K may be obtained [102].

It should be emphasized that high Curie temperatures occur in nominally highly diluted magnetic systems, where the magnetic impurity fraction in the nonmagnetic semiconductor matrix can be 0.4–5 at.%, Therefore, the observed effects, at first glance, are quite difficult to describe satisfactorily using the conventional magnetic exchange mechanisms. Some theoretical studies argue that the magnetic interaction in this case is a consequence of the well-known indirect Zener exchange via band carriers [13, 98]. In this case, manganese impurity, which provides hole doping, is usually considered. An increase in the hole concentration causes an increase in the exchange integral, and, consequently, the Curie temperature T_C should increase with increasing manganese concentration in the film [13, 98]. If, in addition, the exchange energy values are selected properly, then Curie temperatures close to those observed experimentally can be obtained [13, 98]. It is interesting that this coherent theoretical picture completely contradicts the experiment for Si⟨Mn⟩ films, where the maximum T_C value appears at the minimum manganese content [94]. To explain the high T_C values, in a number of cases, the concept of specific structural phases of compounds arising in the semiconductor matrix upon the introduction of magnetic impurities has been invoked [99–102]. However, with this approach, it remains unclear why these new structural phases have a high Curie temperature.

The importance of searching for a mechanism for enhancing the magnetic interaction and taking into account the influence of magnetic inhomogeneities in this class of materials was noted in [95, 96], where Si⟨Mn⟩ films were studied. According to [95, 96], the increase in T_C in this system occurs as follows. During synthesis, the manganese impurity is distributed nonuniformly in the sample and, as a result, inclusions of silicides of complex composition with metallic conductivity are formed as nanometer-sized clusters in the semiconductor matrix. The localized magnetic moments of manganese in the clusters should interact via the RKKY mechanism with $T_{C0} \sim 10$ K. However, strong spin fluctuations change the dependence of the exchange integral J on the distance between the LMMs. As a result, the ferromagnetic transition temperature is renormalized and can be estimated as the geometric mean of the initial Curie temperature for the standard RKKY function and the electron band width W: $T_C = \sqrt{T_{C0}W}$ [95, 96]. Considering that $W \sim 10^4$ K, one would expect T_C values of ~ 300 K to be in reasonable agreement with experiment. Within the framework of this approach, it is difficult not to see an analogy with $Mn_{1-x}Rh_xSi$ samples, where the magnetic subsystem has a cluster character and spin fluctuations can play a significant role. However, the explanation of the large T_C values in [95, 96] is a typical example of an *ad hoc* theory that was not developed further. It remains unclear to what extent these results can be generalized to the case of other magnets and, in particular, to the cases of $Mn_{1-x}Rh_xSi$ or the magnetic phases of GaSb⟨Mn⟩ and GaSb⟨Cr⟩.

It should be noted that any mechanism of magnetic exchange or its enhancement must be 'designed' in such a way that it can overcome the tendency for T_C to decrease due to disorder, since it has long been established that dilute magnetic semiconductors represent Griffiths phases [14]. However, this fundamental circumstance is completely ignored in existing theories [13, 95, 96, 98], and at present it is impossible to say to what extent the results of studying such

materials can help understand the nature of the anomalous increase in T_C in $Mn_{1-x}Rh_xSi$.

Interestingly, the effect of increasing T_C can be obtained in the spin-polaron model if spin polarons are considered as renormalized LMMs forming a ferromagnetic phase. If we assume that the main influence is exerted by the change in the magnetic moment of the spin polaron, the value of J changes little and the influence of disorder can be neglected, then, using the well-known general relationship $T_C \sim J\mu^2$ [22, 66], we can expect an increase in the Curie temperature with a change in the magnetic state of the spin polaron:

$$\frac{T_C}{T_{C0}} \sim \left(\frac{\mu_{0+}}{\mu_{0-}}\right)^2 \sim 40\,. \tag{27}$$

In the experiment, T_C for $Mn_{1-x}Rh_xSi$ increases by no more than 7–12 times, therefore, an estimate (27) apparently means that in this case the effects of disorder in the Griffiths phase are not small, but the renormalization of the magnetic moment in the clusters turns out to be sufficient to ensure the observed gigantic increase in the Curie temperature.

Thus, explaining the effects of a giant increase in the Curie temperature proves to be a highly complex task. The rise in T_C is particularly challenging to explain because it occurs in Griffiths-type systems with strong magnetic disorder. Until recently, it was generally believed that disorder unambiguously leads to the suppression of the magnetic transition. However, the experimental examples presented in this paper demonstrate that disordered magnetic systems may have mechanisms that make it possible to overcome the limitations characteristic of the Griffiths phases. In general, the resulting Curie temperature can be influenced by various factors in addition to magnetic disorder, including changes in the exchange integral J and the effective magnetic moment μ, as well as modifications to the dependence of the magnetic interaction on spatial coordinates. Varying these parameters can, in principle, lead to either an increase in T_C or a decrease in the ferromagnetic transition temperature that likely explains the different dependences of the Curie temperature on the concentration of impurity atoms. The unique case of rhodium impurity in manganese monosilicide also requires further clarification of the nature of the giant increase in T_C and the microscopic mechanism that causes this unusual phenomenon.

6. Conclusion

In this paper, we demonstrated that the type of magnetic disorder we considered in Griffiths systems, namely the dispersion of local magnetic fields generated by spin clusters, occurs in various experimental systems with ferromagnetic interactions and determines their magnetic characteristics. A striking manifestation of this type of disorder is the power-law field dependence of magnetization in the ferromagnetic Griffiths phase, which can be observed over wide ranges of temperature and magnetic field. Analysis of the power-law functions $M(H)$ allows the construction of an order parameter for the Griffiths phase, in which a finite magnetic transition temperature is maintained. These results not only can be viewed as expanding the Griffiths phase paradigm but also are of interest for the development of the theory of critical phenomena. Indeed, since the mid-1970s, following the work of Imry and Ma [103], it has been accepted that "the influence of a random magnetic field is so great that for $d \leqslant 4$ (here d is the dimension of space — author's note) the occurrence of finite magnetization is impossible, and it does not matter how weak this field is, as long as it is not zero" ([38], p. 211 of Russian edition). At the same time, in a recent work [17], it was established using the Monte Carlo method that the dispersion of the local field in the Griffiths phase does not have a very strong effect on the magnetic properties and only slightly reduces the ferromagnetic transition temperature for the entire system.

The performed analysis of experimental data shows that the well-defined Curie temperature and spontaneous magnetization of ferromagnetic clusters forming the Griffiths phase coexist with random magnetic fields. Such magnetic systems could undoubtedly become an important and interesting subject for further theoretical research.

Our study of recently synthesized $Mn_{1-x}Rh_xSi$ substitutional solid solutions suggests that the standard understanding of the Griffiths phase as a system with a suppressed magnetic transition temperature is not an absolute rule. In the presence of strong disorder associated with local magnetic fields (which should destroy the magnetically ordered phase), the Curie temperature in this compound increases from 29 K ($x = 0$) to $\sim$ 350 K ($x = 0.8$). The observed gigantic (12-fold) increase in the magnetic transition temperature also challenges most existing theories. We have shown that this effect cannot be explained by 'negative chemical pressure.' The attempts to interpret the increase in the ferromagnetic transition temperature within the framework of understanding MnSi as a weak itinerant magnet also appears unsuccessful.

It is interesting that two main explanations for the rise in the Curie temperature are possible. The first explanation relies heavily on clustering of the magnetic subsystem and changes in the dependence of the exchange integral on spatial coordinates under conditions of strong spin fluctuations [95, 96]. In this case, it is the Griffiths phase that actually causes the enhancement of ferromagnetic properties, but only under the condition of the emergence of a new mechanism of magnetic interaction. This possibility is favored by the data on the increase in the Curie temperature in the magnetic field-induced Griffiths phase of $Mn_{1-x}Fe_xSi$.

The second explanation is based on the spin-polaron model [21, 54, 59], where the main 'building blocks' that form the various magnetic phases are quasi-bound states of localized magnetic moments of magnetic ions and itinerant electrons, whose sizes do not exceed the lattice constant. Within the framework of this approach, the increase in the Curie temperature is an elementary consequence of the renormalization of the magnetic moment of the spin polaron, caused by a change in its internal structure. Moreover, this effect is apparently strong enough to overcome the standard suppression of the magnetic transition temperature caused by disorder in the Griffiths phase. Thus, in the spin-polaron model, the 'trivial' giant increase in the Curie temperature arises from the nontrivial organization of the magnetic subsystem on the nanometer scale.

The spin-polaron model, although demonstrating its fruitfulness for describing the magnetic properties of various strongly correlated electron systems, is phenomenological and, for its confirmation, requires a theoretical study of the microscopic mechanisms that ensure the formation of spin polarons and define their internal magnetic structure. This study should be based on the investigation of magnetic correlations on the subnanometer scale of less than 1 nm in

the conditions of a multicenter and multiparticle problem. Moreover, it can be expected that the nanometer scale of ~ 10 nm will correspond to the size of magnetic clusters in the Griffiths phase [4, 7]. Thus, we expect that the study of magnetism on the nanometer scale will prove to be a promising direction for the study of various disordered magnets. It is likely that the solution to this problem will require the development of new theoretical and experimental methods that will give new impetus to the development of the physics of magnetic phenomena. The anomalous increase in the Curie temperature for a number of systems can also find its applications in applied research areas aimed at creating and using new magnetic materials.

Acknowledgements. The authors express their gratitude to A.K. Zvezdin and V.N. Ryzhov for useful discussions and to E.V. Zakharova for assistance in preparing the manuscript. SVD is grateful to D.I. Khomsky for a discussion of the physics of the spin-polaron model, which facilitated the development of this theoretical approach. The analysis of the magnetic properties of Griffiths phases in systems with magnetic disorder, the effect of a giant increase in the Curie temperature in MnSi–RhSi solid solutions, and the development of theoretical models were supported by the Russian Science Foundation grant 22-12-00008-П. Measurements of the heat capacity of manganese monosilicide with rhodium impurity were carried out with the support of the Priority-2030 Strategic Academic Leadership Program of National MISIS University within the framework of the Quantum Internet strategic project.

References

1. Griffiths R B *Phys. Rev. Lett.* **23** 17 (1969)
2. Bray A J *Phys. Rev. Lett.* **59** 586 (1987)
3. Sachdev S *Quantum Phase Transitions* 2nd ed. (Cambridge: Cambridge Univ. Press, 2011) DOI:10.1017/CBO9780511973765
4. Demishev S V, Semeno A V, Ohta H *Appl. Magn. Reson.* **52** 379 (2021)
5. Fisher D S *Phys. Rev. Lett.* **69** 534 (1992)
6. Fisher D S *Phys. Rev. B* **51** 6411 (1995)
7. Demishev S V *Phys. Solid State* **51** 547 (2009); *Fiz. Tverd. Tela* **51** 514 (2009)
8. Brady D et al. *Phys. Rev. Research* **6** 013052 (2024)
9. Reed M E W et al. *Phys. Rev. A* **99** 063611 (2019)
10. Yahalom Y, Shnerb N M *Phys. Rev. Lett.* **122** 108102 (2019)
11. Amaral M A, de Oliveira M M *Phys. Rev. E* **104** 064102 (2021)
12. Juhász R, Kovács I A, Iglói F *Phys. Rev. E* **91** 032815 (2015)
13. Sato K et al. *Rev. Mod. Phys.* **82** 1633 (2010)
14. Galitski V M, Kaminski A, Das Sarma S *Phys. Rev. Lett.* **92** 177203 (2004)
15. Krasnorussky V N et al. *Phys. Rev. Materials* **8** 124405 (2024)
16. Demishev S V et al. *JETP Lett.* **121** 111 (2025); *Pis'ma Zh. Eksp. Teor. Fiz.* **121** 121 (2025)
17. Mallick O *J. Magn. Magn. Mater.* **626** 173045 (2025)
18. Demishev S V *Dokl. Ross. Akad. Nauk. Fiz. Tekh. Nauki* **521** 31 (2025) DOI:10.7868/S3034508125020024
19. Krivoruchko V N, Marchenko M A, Melikhov Y *Phys. Rev. B* **82** 064419 (2010)
20. Pahari R et al. *Phys. Rev. B* **99** 184438 (2019)
21. Demishev S V, Ishchenko T V, Samarin A N *Low Temp. Phys.* **41** 971 (2015); *Fiz. Nizk. Temp.* **41** 1243 (2015)
22. Vonsovskii S V *Magnetizm* (Moscow: Nauka, 1971); Translated into English: Vonsovskii S V *Magnetism* (New York: John Wiley and Sons, 1974)
23. Salamon M B, Lin P, Chun S H *Phys. Rev. Lett.* **88** 197203 (2002)
24. Pramanik A K, Banerjee A *Phys. Rev. B* **81** 024431 (2010)
25. Singh N K et al. *Phys. Rev. B* **81** 184414 (2010)
26. Ślebarski A, Goraus J, Fijalkowski M *Phys. Rev. B* **84** 075154 (2011)
27. Pathak A K et al. *Phys. Rev. B* **89** 224411 (2014)
28. Pathak A K et al. *Phys. Rev. B* **94** 224406 (2016)
29. Harbi A et al. *Phys. Rev. B* **104** 054404 (2021)
30. Silva R S (Jr.) et al. *Phys. Rev. B* **106** 134439 (2022)
31. Silva R S (Jr.) et al. *J. Magn. Magn. Mater.* **546** 168851 (2022)
32. Fita I et al. *Phys. Rev. B* **101** 224433 (2020)
33. Wang W et al. *J. Magn. Magn. Mater.* **529** 167868 (2021)
34. Singh K, Bitla Y, Panwar N *J. Magn. Magn. Mater.* **591** 171716 (2024)
35. Ji X et al. *J. Magn. Magn. Mater.* **519** 167455 (2021)
36. Schroeder A, Ubaid-Kassis S, Vojta T *J. Phys. Condens. Matter* **23** 094205 (2011)
37. Wang R et al. *Phys. Rev. Lett.* **118** 267202 (2017)
38. Ma Sh *Sovremennaya Teoriya Kriticheskikh Yavlenii* (Moscow: Mir, 1980); Translated from English: Ma Sh *Modern Theory of Critical Phenomena* (Reading, MA: W.A. Benjamin, 1976)
39. Castro Neto A H, Castilla G, Jones B A *Phys. Rev. Lett.* **81** 3531 (1998)
40. Chan P Y, Goldenfeld N, Salamon M *Phys. Rev. Lett.* **97** 137201 (2006)
41. Ovchinnikov A S et al. *Phys. Rev. B* **106** L020401 (2022)
42. Eremina R M *Appl. Magn. Reson.* **56** 559 (2025)
43. Demishev S V et al. *Phys. Rev. B* **80** 245106 (2009)
44. Demishev S V et al. *JETP Lett.* **91** 11 (2010); *Pis'ma Zh. Eksp. Teor. Fiz.* **91** 12 (2010)
45. Brando M et al. *Rev. Mod. Phys.* **88** 025006 (2016)
46. Yang R-F et al. *Appl. Phys. Lett.* **90** 032502 (2007)
47. Eremina R M et al. *Phys. Rev. B* **84** 064410 (2011)
48. Seidov Z Y et al. *J. Magn. Magn. Mater.* **552** 169190 (2022)
49. Bauer A et al. *Phys. Rev. B* **82** 064404 (2010)
50. Grigoriev S V et al. *Phys. Rev. B* **83** 224411 (2011)
51. Demishev S V et al. *JETP Lett.* **98** 829 (2014); *Pis'ma Zh. Eksp. Teor. Fiz.* **98** 933 (2013)
52. Demishev S V et al. *Phys. Usp.* **59** 559 (2016); *Usp. Fiz. Nauk* **186** 628 (2016)
53. Janoschek M et al. *Phys. Rev. B* **87** 134407 (2013)
54. Demishev S V *Phys. Usp.* **67** 22 (2024); *Usp. Fiz. Nauk* **194** 23 (2024)
55. Mishra A K et al. *Phys. Rev. B* **107** L100405 (2023)
56. Moriya T *Spin Fluctuations in Itinerant Electron Magnetism* (Springer Ser. in Solid-State Sciences, Vol. 56) (Berlin: Springer-Verlag, 1985) DOI:10.1007/978-3-642-82499-9
57. Demishev S V et al. *JETP Lett.* **93** 213 (2011); *Pis'ma Zh. Eksp. Teor. Fiz.* **93** 231 (2011)
58. Demishev S V et al. *Phys. Rev. B* **85** 045131 (2012)
59. Demishev S V *Appl. Magn. Reson.* **51** 473 (2020)
60. Corti M et al. *Phys. Rev. B* **75** 115111 (2007)
61. Demishev S V et al. *JETP Lett.* **100** 28 (2014); *Pis'ma Zh. Eksp. Teor. Fiz.* **100** 30 (2014)
62. Mühlbauer S et al. *Science* **323** 915 (2009)
63. Tonomura A et al. *Nano Lett.* **12** 1673 (2012)
64. Lobanova I I, Glushkov V V, Sluchanko N E, Demishev S V *Sci. Rep.* **6** 22101 (2016)
65. Neubauer A et al. *Phys. Rev. Lett.* **102** 186602 (2009)
66. Dalmas de Réotier P et al. *Phys. Rev. Lett.* **133** 236502 (2024)
67. Blinov L M *Structure and Properties of Liquid Crystals* (Dordrecht: Springer, 2010) DOI:10.1007/978-90-481-8829-1; Translated into Russian: Blinov L M *Zhidkie Kristally. Struktura i Svoistva* (Moscow: Librokom, 2013)
68. Arrott A, Noakes J E *Phys. Rev. Lett.* **19** 786 (1967)
69. Glushkov V V et al. *Phys. Rev. Lett.* **115** 256601 (2015)
70. Grigoriev S V et al. *Phys. Rev. B* **79** 144417 (2009)
71. Demishev S V et al. *JETP Lett.* **104** 116 (2016); *Pis'ma Zh. Eksp. Teor. Fiz.* **104** 113 (2016)
72. Dhital C et al. *Phys. Rev. B* **95** 024407 (2017)
73. Khvostantsev L G, Slesarev V N, Brazhkin V V *High Press. Res.* **24** 371 (2004)
74. Gerashchenko A P "Spektroskopiya NMR v issledovaniyakh elektronnykh i magnitnykh svoistv sil'no korrelirovannykh sistem" ("NMR spectroscopy in studies of electronic and magnetic properties of strongly correlated systems"), Thesis for Doctorate of Phys. and Math. Sci. (Ekaterinburg: M.N. Mikheev Institute of Metal Physics, Ural Branch of the Russian Academy of Sciences, 2019)

75. Krasnorussky V N, Demishev S V, Bokov A V, Salamatin D A, Semeno A V, Os'kin A E, Brazhkin V V, Tsvyashchenko A V "Magnitnye svoistva $Mn_{1-x}Rh_xSi$ ($x < 0.15$): gigantskoe usilenie ferromagnetizma, nizkotemperaturnaya anomaliya i faza Griffitsa" ("Magnetic properties of $Mn_{1-x}Rh_xSi$ ($x < 0.15$): giant enhancement of ferromagnetism, low-temperature anomaly and Griffiths phase"), in *Soveshchanie po Fizike Nizkikh Temperatur. Sb. Tezisov Mezhdunarodnoi Konf. FNT-2024, 3–7 Iyunya 2024 g., Chernogolovka* (Meeting on Low Temperature Physics: Proc. of the Intern. Conf. FNT-2024, June 3–7, 2024, Chernogolovka) (Ed. B B Straumal) (Chernogolovka: Osipyan Institute of Solid State Physics RAS, 2024) p. 79
76. Yu U, Min B I *Phys. Rev. B* **74** 094413 (2006)
77. Greer A L *Thermochim. Acta* **42** 193 (1980)
78. Babić E et al. *J. Magn. Magn. Mater.* **15–18** 249 (1980)
79. Kanomata T et al. *Mater. Sci. Eng. A* **179–180** 351 (1994)
80. Mendelssohn K *Cryophysics* (New York: Interscience Publ., 1960); Translated into Russian: Mendelssohn K *Fizika Nizkikh Temperatur* (Moscow: IL, 1963)
81. Beille J et al. *J. Magn. Magn. Mater.* **10** 265 (1979)
82. Motokawa M et al. *J. Magn. Magn. Mater.* **70** 245 (1987)
83. Kvasnikov I A *Termodinamika i Statisticheskaya Fizika* (Thermodynamics and Statistical Physics) Vol. 1 *Teoriya Ravnovesnykh Sistem. Termodinamika* (Equilibrium Systems Theory. Thermodynamics) (Moscow: URSS, 2002) p. 98
84. Jin Z et al. *Sci. Adv.* **9** eadd5239 (2023) DOI:10.1126/sciadv.add5239
85. Nagaev E L *Fizika Magnitnykh Poluprovodnikov* (Moscow: Nauka, 1979); Translated into English: Nagaev E L *Physics of Magnetic Semiconductors* (Moscow: Mir Publ., 1983)
86. Usachev P A et al. *Mater. Horiz.* **12** 512 (2025)
87. Demishev S V et al. *Solid State Commun.* **385** 115501 (2024)
88. Shklovskii B I, Efros A L *Elektronnye Svoistva Legirovannykh Poluprovodnikov* (Moscow: Nauka, 1979); Translated into English: Shklovskii B I, Efros A L *Electronic Properties of Doped Semiconductors* (Springer Series in Solid-State Sciences, Vol. 45) (Berlin: Springer-Verlag, 1984) DOI:10.1007/978-3-662-02403-4
89. Moriya T "Recent progress in the theory of itinerant electron magnetism" *J. Magn. Magn. Mater.* **14** 1 (1979); Translated into Russian: Moriya T "Poslednie dostizheniya teorii magnetizma kollektivizirovannykh elektronov" *Usp. Fiz. Nauk* **135** 117 (1981)
90. Zhang F M et al. *Appl. Phys. Lett.* **85** 786 (2004)
91. Bolduc M et al. *Phys. Rev. B* **71** 033302 (2005)
92. Liu X C et al. *J. Appl. Phys.* **100** 073903 (2006)
93. Liu X C et al. *J. Appl. Phys.* **102** 033902 (2007)
94. Ko V et al. *J. Appl. Phys.* **104** 033912 (2008)
95. Men'shov V N et al. *Phys. Rev. B* **83** 035201 (2011)
96. Aronzon B A et al. *Phys. Rev. B* **84** 075209 (2011)
97. Xie Z et al. *Phys. Rev. B* **109** 024407 (2024)
98. Dietl T, Ohno H *Physica E* **9** 185 (2001)
99. Kondrin M V et al. *JETP Lett.* **84** 195 (2006); *Pis'ma Zh. Eksp. Teor. Fiz.* **84** 228 (2006)
100. Popova S V et al. *Phys. Solid State* **48** 2177 (2006); *Fiz. Tverd. Tela* **48** 2057 (2006)
101. Kondrin M V et al. *J. Phys. Conf. Ser.* **121** 032011 (2008)
102. Kondrin M V et al. *J. Phys. Condens. Matter* **23** 446001 (2011)
103. Imry Y, Ma S *Phys. Rev. Lett.* **35** 1399 (1975)